HHS Public Access

Author manuscript

Neuropsychologia. Author manuscript; available in PMC 2016 September 01.

Published in final edited form as:

Neuropsychologia. 2015 September ; 76: 108–124. doi:10.1016/j.neuropsychologia.2015.03.021.

Laminar Profile of Spontaneous and Evoked Theta: Rhythmic Modulation of Cortical Processing During Word Integration

Eric Halgren[1,*], **Erik Kaestner**[2], **Ksenija Marinkovic**[3], **Sydney S. Cash**[4], **Chunmao Wang**[5], **Donald L. Schomer**[5], **Joseph R. Madsen**[6], and **Istvan Ulbert**[7]

[1]Departments of Radiology and Neurosciences, University of California at San Diego, La Jolla, California 92069

[2]Interdepartmental Neurosciences Program, University of California at San Diego, La Jolla, California 92069

[3]Department of Psychology, San Diego State University, San Diego, California

[4]Department of Neurology, Massachusetts General Hospital, Harvard Medical School, Boston, Massachusetts 02129

[5]Department of Neurology, Beth Israel Deaconess Medical Center, Harvard Medical School, Boston, Massachusetts

[6]Department of Neurosurgery, Children's Hospital, Harvard Medical School, Boston, Massachusetts

[7]Institute of Psychology, Hungarian Academy of Sciences, Budapest, Hungary

Abstract

Theta may play a central role during language understanding and other extended cognitive processing, providing an envelope for widespread integration of participating cortical areas. We used linear microelectrode arrays in epileptics to define the circuits generating theta in inferotemporal, perirhinal, entorhinal, prefrontal and anterior cingulate cortices. In all locations, theta was generated by excitatory current sinks in middle layers which receive predominantly feedforward inputs, alternating with sinks in superficial layers which receive mainly feedback/associative inputs. Baseline and event-related theta were generated by indistinguishable laminar profiles of transmembrane currents and unit-firing. Word presentation could reset theta phase, permitting theta to contribute to late event-related potentials, even when theta power decreases relative to baseline. Limited recordings during sentence reading are consistent with rhythmic theta activity entrained by a given word modulating the neural background for the following word. These findings show that theta occurs spontaneously, and can be momentarily suppressed, reset and synchronized by words. Theta represents an alternation between feedforward/divergent and associative/convergent processing modes that may temporally organize sustained processing and

* Correspondence should be addressed to EH (ehalgren@ucsd.edu).

optimize the timing of memory formation. We suggest that words are initially encoded via a ventral feedforward stream which is lexicosemantic in the anteroventral temporal lobe; its arrival may trigger a widespread theta rhythm which integrates the word within a larger context.

Keywords

Entorhinal; inferotemporal; prefrontal; perirhinal; cingulate; feedforward; feedback; current-source density; gamma; delta; memory; language

Introduction

Visual and auditory words evoke a progression of activity along their respective ventral streams from sensory cortices, through grapheme and phoneme wordform encoding, to the anteroventral temporal lobe (AVTL). The ‘hub’ theory of word understanding posits that the AVTL then organizes lexico-semantic access (Patterson et al., 2007), a prerequisite for integration with the cognitive context. This progressive activation has been localized with hemodynamic studies, and its importance has been demonstrated in neuropsychological studies, as described in this Special Issue.

Magnetoencephalography (MEG) and electroencephalography (EEG) can be used to time different components of this progressive activation (Halgren et al., 2002b; Marinkovic et al., 2003; Thesen et al., 2012; Travis et al., 2013). MEG and EEG studies average event-related activity with respect to the stimulus to create Event-Related Fields and Potentials (ERPs). ‘Components’ are identified in ERPs as consistent constellations of latency, polarity, topography, and task correlates, which can be studied in multiple populations and conditions. The N400 component has been associated in many studies with lexico-semantic encoding (Kutas and Federmeier, 2011). It is largest to isolated words, and is attenuated by semantic or repetition priming (Halgren, 1990). The N400 is evoked by words in any modality (Marinkovic et al., 2003; Leonard et al., 2012), from an early age (Travis et al., 2011). Definitive localization of N400 generators requires intracranial recordings directly from the human brain, which sometimes occur in order to localize seizure onset prior to surgical treatment. Such studies have identified the AVTL as the most prominent N400 generator, within a network that also includes cortex in or near Broca's and Wernicke's areas (Smith et al., 1986; Halgren et al., 1994a; Halgren et al., 1994b; Nobre and McCarthy, 1995).

Although intracranial local field potential (LFP) recordings provide excellent spatial and temporal resolution, they provide limited information regarding the synaptic circuitry underlying these components because neither the polarity nor the amplitude of LFP, MEG or EEG signals has any necessary correlation with the level of neuronal activity (Halgren, 2008). However, the broadband high gamma power (HGP) calculated from the LFP is highly correlated with local neuronal firing (Lachaux et al., 2012). HGP increases during the AVTL-N400, with similar task correlates, indicating that the AVTL-N400 reflects neuronal excitation (Chan et al., 2011).

Intracranial studies also found that the AVTL-N400 and the associated HGP respond differentially to words referring to animals versus objects, with different recording sites showing preferences for one or the other semantic word category (Chan et al., 2011). Microelectrode recordings found that neurons in the medial temporal lobe may fire to particular words during the N400 (Heit et al., 1988, 1990). Furthermore, both spoken and written words were found to activate the same sites with the same semantic preferences, supporting the proposal that the AVTL comprises a supramodal semantic hub for word understanding.

The synaptic circuitry generating the N400 has been inferred using Current Source Density (CSD) estimated using 'laminar electrodes' in AVTL (Halgren et al., 2006). Laminar electrodes are linear arrays of microelectrodes sampling LFP in different layers of a cortical column (Ulbert et al., 2001). CSD measures the currents across neuronal membranes, which can be produced by excitatory and inhibitory synaptic activity or voltage-gated channels (Nicholson and Freeman, 1975). Since synaptic inputs from different destinations arrive in different cortical layers, CSD can be used to infer the circuitry underlying the N400. The initial response to words in AVTL is a sink in layer IV with increased unit firing and peaking at ~200ms and associated with the N200 component (Halgren et al., 2006). An initial excitatory layer IV sink is the typical pattern produced by feedforward input from lower (i.e., more sensory) to higher cortical areas (Felleman and VanEssen, 1991; Salin and Bullier, 1995; Barbas and Rempel-Clower, 1997). The initial layer IV sink occurs to words occurring for the first time in a task ('new') and to those that have been repeated many times ('old'). However, the layer IV sink to old words quickly returns to baseline while the response to new words continues. The timing and task correlates of this divergence is similar to that of the scalp N400, implying that the N400 is an extended feed forward sink in layer IV (Halgren et al., 2006).

In summary, the AVTL-N400 is generated by the first-pass (feedforward) supramodal lexico-semantic encoding of words, and thus is a reasonablen excellent candidate for the initial activity in what some consider to be a semantic hub. Ultimately, the role of the AVTL in lexico-semantic encoding will only be resolved through the construction of mechanistic models which combine these electrophysiological studies with hemodynamic and lesion studies. However the averaging process used to construct ERPs eliminates the great majority of the LFP, not only that in the baseline, but also much that is related to the event but is not timelocked to the stimulus (Makeig et al., 2002). Neither pre-word activity, nor long latency activity is typically time-locked to the stimulus, and therefor both are lost during averaging. The view provided by ERPs is thus incomplete, neglecting the preceding baseline which provides the context for processing, as well as the subsequent extended activity, which supports the integration of the word into discourse.

In order to explore non-time-locked activity, single trials are typically quantified in the frequency domain. EEG and MEG display prominent high delta and low theta activity (3-6Hz) in a variety of tasks requiring extended processing, working memory and executive control (Kovacevic et al., 2012; Hsieh and Ranganath, 2013). Source estimation, confirmed by intracranial recordings, indicate prominent generators in the anterior cingulate (AC) and dorsolateral prefrontal (PF) cortices (Wang et al., 2005; Cavanagh et al., 2012; Kovacevic et

al., 2012). EEG and MEG theta are also associated with verbal and nonverbal memory retrieval (Klimesch, 1996; Bastiaansen and Hagoort, 2003; Marinkovic et al., 2012), and spatial processing (Snider et al., 2013), corresponding to the correlates of theta in the hippocampus and related structures in rodents (Hasselmo and Stern, 2013). In these tasks, intracranial studies in humans suggest widespread theta generation (Halgren et al., 2002a; Raghavachari et al., 2006; Rizzuto et al., 2006; Knake et al., 2007; Steinvorth et al., 2010; Fell and Axmacher, 2011; Lega et al., 2011). Furthermore, human cortical theta modulates HGP (Canolty et al., 2006), and presumably neuronal firing (Lachaux et al., 2012). Thus, the theta rhythm in humans appears to be an active process that modulates widespread areas of the cortex during sustained processing in multiple cognitive tasks.

Here we examine single trial activity recorded with linear microelectrode arrays in the AVTL. The potential gradient (PG) within and between cortical layers was recorded during visual word processing using 23 pairs of microcontacts spanning ~3.5mm of inferotemporal (IT), perirhinal (PR), entorhinal (ER), prefrontal (PF) and anterior cingulate (AC) cortices. Laminar CSD profiles were estimated from PG using standard methods (see below). For each site, we examine three issues: theta involvement in cognitive processes as indexed by event-related modulation; synaptic generation of theta revealed by CSD and multi-unit activity (MUA) in different cortical layers; and identity of theta generation in the pre-stimulus versus post-stimulus periods by comparing their laminar CSD/MUA profiles.

We find that the feedforward time-locked activity giving rise to the N200/N400 can be clearly evident on single trials in the AVTL, but that the predominant activity is low theta/high delta activity. Theta activity dominates the baseline; word input evokes a layer IV sink which resets and synchronizes the theta. This synchronization results in theta contributing to averaged LFPs despite an overall decrease in theta power. Theta is generated by a layer IV sink with increased neuronal firing, alternating with a layer II/III sink. Baseline and event-related theta have identical generators. Outside of the AVTL, in prefrontal and cingulate cortices, the initial sharp layer IV sink was not observed but theta with the same laminar generation pattern was. These findings suggest that words are initially encoded via a ventral feedforward stream which is lexicosemantic in the AVTL; its arrival may trigger a widespread theta rhythm which integrates the lexicosemantic content within a larger context. Limited recordings during sentence reading are consistent with rhythmic theta activity entrained by a given word modulating the neural background for the following word.

Materials and Methods

Subjects and Probes

Five patients with long-standing pharmaco-resistant complex partial seizures (4 male, average age 30 year; all right handed, with normal intelligence and personality) participated after fully informed consent monitored by institutional review boards at Beth Israel Deaconness Medical Center and Childrens Hospital. Patients 1-3 and 5 were implanted with depth electrodes in order to localize their seizure focus and thus direct surgical treatment. Clinical electrodes were modified to be smaller diameter (350μ) in a 5 mm segment at their tips, containing 24 90%Pt-10%Ir contacts, each 40μ in diameter, at 150μ center-to-center spacing (Ulbert et al., 2001). Recording sites were localized on MRIs taken with the probes

in place (figures 1, 3, 4, and 6). Laminar contacts in gray matter, white matter, and CSF have characteristic activity patterns, permitting resolution of their entry and exit points. Structural MRI and/or histological examination of the surgical specimen was normal except for right hippocampal sclerosis in pt. 3 and compensated aqueductal stenosis in pt. 5. Seizure onset was found to lie outside of the locations reported here: right frontal in patients 1 and 2; right amygdala in patient 3, and right hippocampus and orbitofrontal cortex in patient 5. Patient 4 was implanted with subdural grids for clinical presurgical evaluation. The microarray was placed under the grid in cortex that had been previously identified as probably epileptogenic, in the center of the likely surgical target in the left superior frontal gyrus. The decision to implant, the electrode targets, and the duration of implantation were made entirely on clinical grounds without reference to this study.

Recordings

Differential recordings were made from 23 pairs of successive contacts. After wideband (DC-10,000 Hz) pre-amplification (gain 10×, CMRR 90db, input impedance 10^{12} ohms), the signal was split into field potentials (PG, filtered at 0.2–500 Hz, gain 1,000×, digitized at 2,000 Hz, 16 bit) and action potentials (filtered at 200–5,000 Hz, gain 1,000×, digitized at 20,000 Hz, 12 bit), and stored continuously with stimulus markers. Population trans-synaptic current flows were estimated using Current Source Density (CSD) analysis (Nicholson and Freeman, 1975; Mitzdorf, 1985). CSD was calculated as the second spatial derivative of field potentials (0.5-30Hz) after applying a 5-point Hamming filter (Ulbert et al., 2001).

When CSD current sinks are generated by EPSCs, they generally are accompanied by passive return current sources (Nicholson and Freeman, 1975). Conversely, at the expected membrane potential of cortical neurons in active humans, IPSCs could produce active current sources, and they would be accompanied by a passive current sink. Simultaneous MUA was used to distinguish active synaptic from passive return currents. Population neuronal firing (MUA) was estimated by rectifying high frequency activity (300-3000Hz) and smoothing with a 50hz low pass filter (Ulbert et al., 2001). MUA was not recorded in Pts. 1 and 5 due to interference from the clinical telemetry system. MUA in pt. 3 did not show significant correlations with theta.

Both CSD and MUA decline steeply with distance. Our simulation model indicates that CSD amplitude declines ten fold in ~250μ parallel to the cortical surface and more steeply perpendicular to the surface (Wang et al., 2005). Theoretical and empirical studies in animals indicate that MUA should decline with distance at least as rapidly. Thus, CSD and MUA estimate activity of neurons in a volume roughly corresponding to that of a cortical column. Event-related averages from pts. 1-3 are presented in (Halgren et al., 2006) and (Chan et al., 2011), and from pt. 5 in (Wang et al., 2005).

Spectral Analysis

For each site, several techniques were used to appreciate the distribution, generation, temporal evolution and task-modulation of PG or CSD at different frequencies. Overall spectral power was calculated using an FFT and compared between the first and second sec after stimulus onset in order to qualitatively identify the frequencies present, their general

distribution in different cortical layers, and their general reactivity to behavioral manipulations. The temporal evolution of task-modulation was examined in more detail by calculating on every trial the spectral power for each latency, frequency and cortical depth using complex Morlet's wavelets (Lachaux et al., 1999), then averaging across trials to produce the individual trial event-related spectral power (iERSP) (Halgren et al., 2002a). Relatively constant temporal and frequency resolution across target frequencies was obtained by adjusting the wavelet widths according to the target frequency. The wavelet widths increase linearly from 1 to 6.5 cycles as frequency increases from 1 to 13 Hz, and then remain 7 cycles from 14 to 50Hz (Wang et al., 2005).

When expressed as a z-score relative to the pre-stimulus baseline, iERSP allows the task-related modulation of theta over time to be examined and compared to other frequencies. Deviations relative to baseline can be associated with a probability using the normal distribution because each plot combines the data from ~150-400 trials. Due to the large number of points in the comparison matrix, a threshold of $p<10^{-5}$ was used. Similarly, the two-sample t-test between trials under different cognitive conditions reveals the spatiotemporal effects of that manipulation in different cortical layers. These statistics comparing conditions are plotted for patient 1 in figure 1e3, and similar plots were obtained for other patients. All comparisons noted in the figures or text were significant at $p<10^{-5}$.

Since the absolute levels of spectral power vary greatly across frequencies and cortical layers, the z-score is usually calculated relative to the baseline values for a particular frequency and laminar contact. However, in order to appreciate which layers are contributing relatively more power at different times, iERSP is also plotted as a z-score relative to baselines from all channels combined.

In pt. 3. phase-locking was also calculated between different cortical layers (Lachaux et al., 1999). This measure is sensitive to the similarity of timing in a particular frequency range between two structures, regardless of their amplitudes. Phase-locking of the CSD or PG to stimulus onset was quantified using Inter-Trial Coherence (ITC) with statistical significance evaluated using a bootstrap method (Delorme and Makeig, 2004). All indicated ITC responses are significant at $p<0.01$, approximately corresponding to an ITC value of 2.5.

In order to appreciate the laminar distribution of current sources and sinks generating theta activity, it is necessary to average theta activity with respect to a constant phase. In pts. 1 and 2, the Hilbert transform on data filtered to pass only the theta band was used to obtain a continuous measure of phase (Link et al., 2002). Unfiltered CSD from all channels was averaged with respect to times where phase was $-\pi$. CSD laminar profiles were compared between the 2nd, 3rd and 4th theta cycles prior to the stimulus, and the 2nd, 3rd and 4th theta cycles after the stimulus. In pts. 3-5, the signal-to-noise ratio was not adequate to use this strategy, so theta phase detected by using peak detection on data filtered to pass only the theta band. Peaks were selected in a 400ms interval offset by 100ms from word onset in either direction. Unless otherwise noted, theta peaks were identified in layer III/IV.

The theta peaks identified in this manner were also used to determine phase-amplitude coupling with higher frequencies. Amplitudes in different layers and frequencies (1-200Hz)

was estimated using the Hilbert transform and plotted from −512 to 512ms. Plot are masked to only show those TF locations with a zscore of 3 indicating an uncorrected p<.01, relative to a baseline from −1000 to −500ms.

Tasks

Subjects viewed single words presented on a computer monitor in Geneva font as white letters on a black background in the central ~5% of visual angle. Stimulus exposure was 240ms and stimulus onset asynchrony was 2400ms unless otherwise noted. The monitor was controlled, and keyboard response accuracy and latency were monitored, by MacProbe software (Hunt, 1994). Subjects remained in their hospital room under videotelemetry during the recordings.

Explicit word recognition memory was probed with:

Word Recognition (WR)—Initially, the subject thrice studied 10 words, with instructions to memorize. These words were then presented 12 times each, randomly intermixed with 120 novel words. Word length was 5.20±.75 (mean ± standard deviation) letters, and lexical frequency was 4.18±4.92 (Word frequency was obtained from MCWord, http://www.neuro.mcw.edu/mcword/, which is based on the CELEX database: Medler, D.A., & Binder, J.R., MCWord: An On-Line Orthographic Database of the English Language. 2005). Any given word repeated after an average delay of ~50 s and ~20 intervening stimuli. Subjects were instructed to press a key with their dominant hand within 1200 ms after presentation of a repeating word. At 1360 ms post-stimulus, a 55ms feedback tone indicated whether the response (or lack thereof) had been correct (1000 Hz) or wrong (200 Hz). Performed by pts. 1-3 and 5. Pts. 2, 3, and 5 performed correctly on 96, 98 and 96% of the trials, with reaction times of 762 ±204, 850 ±121, and 756 ±214ms. Behavioral results from pt.1 were not available. In an identical task, large potentials were recorded in the ventral temporal lobe using depth macro-electrodes in epileptic patients (Halgren et al., 1994a).

Incidental word repetition was probed with two tasks:

Size Judgment (SJ)—The subject pressed a key if the object or animal that the word represents is usually more than one foot in its longest dimension; half of the stimuli were words that repeated several times; 320 stimuli were presented. Word length was 6.38±1.77 letters for words referring to objects, and 6.14±1.74 letters for words referring to animals. Lexical frequency = 5.02±5.85 for words referring to objects, and 4.25±6.02 for words referring to animals. Words referring to objects vs. animals did not differ significantly in either length or lexical frequency (p>.3). Performed by all patients; data is shown for pts. 1, 2 and 4; similar results were obtained in pts. 3 and 5. Behavioral results from this group are not available. However, in the identical task, a group of young normal subjects responded correctly to 92% of the trials at a latency of 960±123ms to new words and 760±81ms to old words, demonstrating strong behavioral priming (Marinkovic et al., 2003). Both MEG and fMRI show ventral temporal activation in the identical task (Dale et al., 2000; Marinkovic et al., 2003).

One subject also performed *Sentence Reading (SR)* comprising 130 sentences, half with 11 words and half with 13. Words were presented individually and foveally with an SOA of 330ms. Approximately 3 seconds passed from the offset of the last word of one sentence to the onset of the next sentence. The patient was instructed to read the sentences carefully for meaning. Half of the sentences ended with a congruent final word, and half with an incongruent word. Not including the first or last word in the sentence, there were 952 content words (length = 5.53±1.92 letters, lexical frequency = 301±11401), and 827 function words (length = 2.88±1.17 letters, lexical frequency = 219445±23777). Content and function words different significantly in length and frequency ($p<.001$). In order to compare the responses of function words with differing predictions for the syntactic category of the subsequent word, two groups of words were assembled. Function words in the first group (termed 'F-c') were usually followed by a content word (95% of cases in these data). Examples of words in this group are: every, the, some, his. Function words in the second group (termed 'F-f') were usually followed by a function word (80% of cases in these data). Examples of words in this group are: because; when, out, off. F-c words (n=110) were 3.38±1.92 letters long, with a lexical frequency of 24927±28122; F-f words (n=150) were 3.25±1.40 letters long, with a lexical frequency of 6108±5350. These groups did not differ significantly in length ($p>.3$), but did differ in frequency ($p<.001$).

Results

One-dimensional transcortical CSD provides an estimate of the current flowing across neural membranes in each cortical layer (Nicholson and Freeman, 1975). Excitatory post synaptic currents (EPSCs) are comprised of positive ions flowing into neurons, i.e., CSD sinks (Figure 8C). Similarly, inhibitory post synaptic currents (IPSCs) are comprised of negative ions flowing into neurons (or equivalently positive ions flowing out), i.e., CSD sources. Current which enters the neuron at the active synapse returns at locations determined by the neuron's morphology and cable properties. Thus, active sinks are associated with passive sources, and active sources with passive sinks. In order to determine if recorded sinks were active or passive we correlated them with simultaneous measures of overall neural activity, HGP and MUA.

Anteroventral Inferotemporal cortex (IT)

PG within and between cortical layers was recorded during delayed word recognition using 23 pairs of microcontacts spanning ~3.5mm of IT (MRI in Figures 1A, S1a). Spontaneous background activity is dominated by delta (1-3 Hz) and theta (4-8 Hz) oscillations in middle to upper cortical layers (Figure 1B, longer sweep in Figure S1b). Word presentation suppresses lower frequencies (gray background).

PG is proportional to extracellular currents between cortical layers that result when there is localized synaptic activity. In contrast, CSD is sensitive to trans-membrane synaptic currents within the layer where they are actually generated, at an accuracy of <250μ (Wang et al., 2005). Plots of CSD power across different frequencies and cortical depths show that theta oscillations (at ~4-5Hz) are maximally generated in middle and superficial cortical layers (Figure S1c). This pattern is seen both during the first sec after word presentation, when the

patient is performing the task, and in the following sec, after the patient has responded and is resting between trials. Greater temporal resolution is obtained in the individual trial event-related spectral power (iERSP) by calculating CSD power on every trial for each latency, frequency and cortical depth, averaging across trials, and normalizing to the same baseline for all channels (Figure S1d). The same middle and superficial layer channels that show relatively greater theta power during the baseline period also appear to be the sites of event-related increases and decreases. Event-related changes are emphasized in Figures 1C and S1e by displaying iERSP as a z-score relative to the baseline for each channel as well as frequency. Starting at ~130ms, there is a broadband burst of spectral power that ends at ~230ms to old words, but continues until ~300ms to new words. Theta then *decreases* compared to baseline until ~800ms, especially to new words. Finally, until ~1300ms, theta increases, especially to old words in middle and deep layers. Thus, word-presentation evokes a complex sequence of theta increases and decreases, which are modulated by repetition in both overt and implicit memory tasks.

CSD waveforms from individual trials had sufficient signal-to-noise ratio to show clear event-related changes (Figure 1D). Pre-stimulus CSD was relatively large, and dominated by low frequencies with no discernable phase-relationship to stimulus onset. Word onset abruptly terminated this activity. A sharp middle layer sink peaking at ~180ms was followed by synchronous theta oscillations that were more prominent for old words. The initial peak was ~100ms in duration to old words, and ~200ms to new (Figure 1H), but included sharper components, and thus contributed to the broadband event-related spectral increase observed in the iERSP (Figure 1C). Theta source peaks were visible at ~300 (to old words only), and ~500 and ~700ms (to both new and old words), after which the theta rapidly lost its phase-locking with the stimulus. These inferences from visual inspection of individual waveforms were confirmed and quantified using inter-trial coherence (ITC). ITC was elevated above baseline from ~100-700ms, especially to old words, but only in the delta and theta frequencies (Figure S1g). The same phenomenon was seen when instantaneous phase was extracted using the Hilbert transform and averaged with respect to stimulus onset (Figure 1G).

Phase-resetting aligns the post-stimulus CSD waves so that traditional averaging methods reveal an evoked response with strong theta oscillations (Figure 1H) even though theta power had decreased from the pre-stimulus period. This post-stimulus alignment allows examination of whether theta phase is related to local information-processing. The F statistic was used to characterize the timecourse of selectivity in local transmembrane currents for different categories of words (Figure S1f). Selectivity oscillated at theta frequency in exact alignment with the middle layer sources and superficial sinks that generate theta. Thus words, and word repetition, not only modulate ongoing theta power, they also ‘take over’ theta in the sense of synchronizing theta phase to stimulus onset, and conversely, theta phase is tightly coupled to the information-selectivity of local synaptic selectivity.

In order to examine the effect of the initial sharp middle layer sink on theta phase-resetting, old word trials were sorted into those with large versus small middle layer sinks at ~190ms. Following the initial broadband burst, similar levels of theta ITC (Figure S1h), and similar late theta oscillations in the averaged CSD (Figure S1i), were observed for the two trial

types. Thus, the local initial middle layer sink does not play a critical role in resetting theta. These averages did reveal a small but significant middle layer source at ~140ms that presumably represents a spontaneous local hyperpolarization present when bottom-up input arrives. It is possible that such hyperpolarization increases the transmembrane current evoked by excitatory synaptic input through de-inactivation of voltage-gated channels, as well as by increasing the difference between the membrane potential and cation reversal potentials.

Details of theta generation were examined by plotting CSD against time in different cortical layers (Figure 1E), or at peak amplitude against cortical depth (Figure 1F). One phase of theta is generated by a middle layer current sink with synchronous sources in superficial, and weakly, deeper layers. This alternates with a phase of theta generated by a superficial sink and middle layer source (Figure 1E). Thus, theta is generated through alternating sources and sinks in middle and superficial cortical layers. High frequency power (HGP) increased at the time of the middle-layer theta sink (Figure 1I), indicating that the middle layer sink is an active EPSC.

Theta amplitude profiles were calculated separately for theta activity prior to the stimulus (i.e., occurring spontaneously), versus after the stimulus (i.e., event-related, due to the phase-reset shown in panels D and G). Theta amplitude profiles across cortical layers were identical for theta cycles recorded before versus after the stimulus (Figures 1E, 1F), demonstrating that event-related and spontaneous thetas are generated by the same intracolumnar current sources and sinks, and by implication, the same synaptic circuitry. CSD depth profiles of event-related theta to new versus old words are also indistinguishable at this very high level of spatiotemporal resolution.

Perirhinal cortex (PR)

Spectral activity in PR (Figures 2, S2) was broadly similar to that in IT. Spontaneous background PG activity between trials (Figure 2B; longer sweep in Figure S2b) showed large delta-theta oscillations, especially in middle cortical layers. Presentation of new or old words suppressed theta; CSD theta power was largest in middle and superficial layers (Figure S2c).

Words evoked a strong broadband increase in PR spectral power from ~130-300ms, earliest in putative layer IV, but rapidly spreading to superficial and then deep layers, which was similar across tasks WR and SJ (Figures 2C, S2d). This initial burst was followed by sustained broadband activity until ~700-800ms, especially in middle and deep layers. During this stage, theta in upper layers profoundly decreased compared to baseline, especially to new words. Both the initial broadband response and the later theta response discriminated between words referring to objects versus animals (Figure 2C), as has been observed in this area for MUA and HGP (Chan et al., 2013).

Superimposed recordings from single trials showed large theta activity with random phase in the pre-stimulus period, reset with a sharp deflection peaking at ~140ms in the middle cortical layers, then a single large synchronized theta frequency oscillation, and recovery by ~1200ms (Figure 2D). The sharp peak was ~100ms duration, corresponding to the ITC alpha

synchronization at ~150ms, followed by synchronization in the theta range (Figure S2e). Theta synchronization was reflected in peaks of averaged Hilbert theta phase at 300, 600 and 800ms (Figure 2G). Phase-locking allowed averaging to reveal an evoked response (Figure 2H), despite the strong decrease in overall LFP amplitude.

As in IT, theta in PR was produced by alternating CSD sinks and sources in middle and superficial cortical layers (Figure 2E). Interpretation of the middle layer sink as an EPSC (with a passive superficial return) was confirmed by the simultaneous increase in population neuronal firing (Figure 2F), and increase in broadband HGP in the spectral power averaged relative to the middle layer theta peak (Figures 2I, S5B). Again, the generating CSD and MUA laminar profiles of spontaneous prestimulus and event-related poststimulus theta rhythms appeared identical (Figures 2E, F).

Entorhinal cortex (ER)

As in IT and PR, laminar probes in ER (Figures 3, S3) recorded an initial wideband increase in spectral power (Figure 3B, S3b). Unlike IT and PR, the broadband increase in ER was larger to old words, the increase began later (at ~280ms for frequencies >10Hz), and extended to higher frequencies (>140Hz). The old>new differences are present in all frequency bands from ~400-600ms after word onset, mainly in superficial layers. After ~600ms, broadband activation declines and spectral increases are mainly <10Hz. Theta increases over baseline for >1000ms.

Perhaps corresponding to ER's unique anatomical structure, plots of overall spectral power versus cortical depth showed separate generators in deep and superficial layers across all frequencies (Figure S3c). Plots of spectral power across time showed that, for both theta and fast rhythms, the same channels are generating activity in the pre-stimulus and post-stimulus periods (Figure S3c). Unlike other areas, theta in ER was generated by both superficial and deep sinks, each with surrounding sources (Figure 3G). The superficial versus deep theta/delta generators became more phaselocked during memory retrieval, as compared to the intertrial interval (Figure 3C).

The superimposed single trial sweeps show, like IT and PR, an initial response followed by a slower wave (Figure 3D). However, the initial response in ER was longer (~340ms, 1.4Hz), as was the following wave (>700ms, <0.7Hz). Furthermore, unlike IT and PR, there was no obvious suppression of background activity following the initial response. This was confirmed by the ITC and the overall average waveform, which were mainly restricted to delta frequencies (Figure 3EF).

The repetition-suppression found in the IT and PR broadband spectral responses is consistent with the repetition-suppression commonly found in macaque unit recordings from the same areas (Brown and Aggleton, 2001). In order to evaluate if ER repetition-enhancement in the current study represents a characteristic property of ER, versus an idiosyncratic response of the subject, macroelectrodes in IT and PR were recorded simultaneously with ER laminars in patient 3 (Figure S3a). Broadband spectral increases in IT and PR began before 200ms, at which time they were not significantly different between new and old words (Figure S3d). Later activity was greater to new words (Figure S3d), i.e.,

showed repetition-suppression, as in the laminar recordings from IT (Figure 1C) and PR (Figure 2C), but unlike the laminar ER recordings in the same subject (Figure 3B). Thus, the long latency repetition-enhancement in laminar ER recordings is probably not a patient-specific abnormal response. This double-dissociation (repetition-suppression in IT and PR, later repetition-enhancement in ER) is consistent with the proposal that ventrolateral temporal areas may be more concerned with simpler forms of memory such as repetition-priming, whereas medial temporal areas may be involved in active retrieval (Brown and Aggleton, 2001).

Dorsolateral Prefrontal Cortex(PF)

As in temporal sites, PF spectral activity was mainly low frequency and generated in upper and middle cortical layers (Figures 4A, S4a). CSD in PF showed the same laminar profile for the theta as in IT and PR: alternating sources and sinks in middle layer, visible in single sweeps (Figure 4B), as well as averaged CSD (Figure 4A). Return currents were mainly in superficial layers. Simultaneous MUA averages (Figure 4D) show that the CSD sinks were associated with increased cell-firing, and thus constituted EPSCs. This was confirmed by broadband spectral power increases at the time of the middle layer theta sink (Figures 4E, S5c).

Event-related and spontaneous theta had identical laminar generating profiles (Figure 4BC). Intertrial coherence was mainly in the delta band (Figure 4G), and the local averaged response is ~1Hz (Figure 4H). Theta power increased and then decreased to words (Figure 4F), with more sustained late theta to old words (Figure S4b). Theta also responded differentially to words referring to animals versus objects (Figure S4c). Unlike temporal sites, no broadband increase to words was observed in PF, only low frequency responses.

Anterior Cingulate Cortex (AC)

Similar patterns were observed for theta generation in AC (Figure 5A). Again, CSD showed the same laminar profile for the theta as in IT and PR: alternating sources and sinks in middle layers, with return currents in superficial layers (Figure 5B). Unlike IT and PR, no initial short latency sharp layer IV sink was evoked, and no broadband increase in spectral power to words was observed. Intertrial coherence was mainly in the delta range (Figure 5C), as was the averaged response (Figure 5D). It was previously reported that theta in this location is larger to old as compared to new words, and to rare target tones compared to frequent non-targets (Wang et al., 2005).

We conclude that spontaneous theta has the same generator as task-evoked, supporting the fundamental identity of these processes. A similar generating profile of oscillating excitation and inhibition was observed in five different cortical areas, confirming that theta reflects a widespread modulation of cortical processing. The focus of excitation appears to alternate between middle and superficial cortical layers, suggesting that theta also reflects an alternating predominance of feedforward versus feedback/associative afferents.

Theta During Sentence Reading

Laminar recordings during reading complete sentences were obtained in PR in Patient 2 (Figure 7). The response to the initial word was similar to that evoked by isolated words in the WR or SJ tasks (Figure 2, {Halgren, 2006 #15569}), comprising an initial middle layer sink with a sharp increase in high gamma power, followed by an upper layer sink and more prolonged increase in HGP (Figure 7ABD). The regular presentation of the words entrains the transmembrane currents in multiple layers at 3Hz, the presentation rate of the words, as well as at 6 Hz in some channels (Figure 7ABC). Oscillatory activity at theta frequency continues for about one second after the end of the sentence (Figure 7ABC). The initial sink to the first word peaks at ~150ms after word onset; the upper layer sink peaks at ~230ms. Later words in the sentence evoke similar activity except for an attenuated initial sink, and the addition of an earlier middle layer sink peaking at ~40-50ms. This peak occurs prior to information concerning the current word, whose arrival is indicated by the initial layer IV sink onset which does not occur before 130ms. Thus, the 40ms peak is triggered by the preceding word and modulates middle layer excitability immediately before information from the current word arrives.

Although content words in sentences evoked responses similar to those evoked by isolated words, function words evoked much attenuated responses, especially in middle layers (Figure 7E), presumably corresponding to the lack of N400m observed with MEG to function words in sentences {Halgren, 2002 #14057}. Some function words (such as ‘out’) are usually followed by another function word, whereas other function words (such as ‘the’) are usually followed by a content word. The peak at 40ms was absent to the former, and large to the latter (Figure 7F), suggesting that the effect of a word on the neural preparation for the next word following it may be modulated by syntactic probabilities.

Discussion

These results show that theta is generated in the human neocortex by a middle layer sink (and superficial source) alternating with superficial sink (and middle layer source). The middle layer sink is correlated with increased neuronal firing and wideband power in multiple layers, and thus is an EPSC. The same generator is observed across widespread cortical sites (Figure 6), with the exception of entorhinal cortex which has two generators. At a high level of spatial and physiological resolution, event-related and spontaneous thetas have identical generators. Event-related theta is strongly modulated by stimulus characteristics and in turn modulates the selectivity of the local neuronal response. Theta phase may be reset by the stimulus so that even if theta power decreases poststimulus, it is still in some locations the major source of the late averaged LFPs. This pattern of theta generation implies an alternation between complementary modes of cortical processing of words and other cognitive stimuli.

Relation of Theta to Intra- and Inter-Columnar Circuitry

The data reported here, together with previous intracranial recordings during recent and working memory tasks (Klopp et al., 1999; Halgren et al., 2002a; Rizzuto et al., 2003; Wang et al., 2005; Canolty et al., 2006; Raghavachari et al., 2006; Rizzuto et al., 2006; Fell and

Axmacher, 2011), conclusively demonstrate that theta is generated in multiple cortical areas, not focally. Although the oscillations in the current study were often slightly slower (3-6Hz) than classical HC theta in rodents (4-8Hz), this is consistent with other findings in humans (Watrous et al., 2013; Jacobs, 2014). Extending previous studies, we found that theta has a similar generating profile in all areas. This suggests that, regardless of cortical location, theta represents the same cognitive processing mode.

Theta in the rodent HC is generated by intrinsic pacemaker (H) currents, organized by local interneurons, and synchronized across areas by the medial septum and other structures (Buzsaki, 2002; Pignatelli et al., 2012; Colgin, 2013). In the awake state, the active currents underlying the HC theta are present in both somatic and dendritic layers (Kamondi et al., 1998; Harvey et al., 2009). Neocortical theta generation is less well understood, but it may involve similar mechanisms, including intrinsic currents (Bilkey and Heinemann, 1999) and parvalbumin-expressing interneurons (Hartwich et al., 2009), with modulation from the HC (Sirota et al., 2008), and from cholinergic and GABAergic cells of the basal forebrain (Jones, 2004).

The current study found that human theta represents current sinks reciprocally oscillating between middle and superficial cortical layers. Anatomically, layer IV receives input from thalamic relay nuclei, or ‘lower’ areas closer to primary sensory cortex (Felleman and VanEssen, 1991; Barbas and Rempel-Clower, 1997). Layer IV cells project locally to other layer IV cells as well as to layer II/III cells (Thomson and Bannister, 2003), forming locally interconnected microcircuits (Yoshimura et al., 2005). The layer II/III pyramids project onward to layer IV of higher cortical areas, as well as locally to layer V/VI pyramids which project back to the superficial layers of lower cortical areas. Superficial layers also receive local recurrent collaterals. These connections define a canonical cortical circuit of convergent feedforward excitation carrying stimulus-specific information to middle cortical layers, and feedback excitation carrying contextual information to superficial layers (Lamme and Roelfsema, 2000; Merker, 2004; Burke et al., 2005). The current data suggest that theta may represent an oscillation between two modes of cortical processing, alternating between periods when predominant excitatory input is feedforward (indicated by a middle layer sink), and periods when top-down and local association afferents predominate (indicated by a superficial sink) (Figure 8).

In our recordings, theta was generated by a single source-sink pair in all cortical areas except ER, where distinct sinks and sources were found in both deep and superficial layers. Phase synchrony between the deep and superficial ER theta generators was low but increased when retrieving well learned memories. This may reflect the fact that the superficial and deep layers of ER have quite distinct anatomical connectivity, and are separated by a cell-free ‘lamina dissecans’ (Insausti and Amaral, 2004). In contrast to these data from human ER, the dominant theta generator in rodent ER is thought to lie in superficial layers, although deep ER pyramidal cells do show theta-range membrane oscillations and theta-correlated unit-firing (Alonso, 2002).

Relation of rhythms to averaged event-related potentials and fields

ERPs are often thought to represent evoked activity superimposed on an unrelated background that is suppressed by averaging. Alternatively, ERPs may arise from phase-resetting of spontaneous EEG rhythms. This possibility is supported by the similar frequency components and scalp topographies of spontaneous EEG and ERPs, and the inter-trial coherence of post-stimulus EEG (Makeig et al., 2002; Cavanagh et al., 2012). However, similar phenomena are found when potentials are superimposed on an unrelated background (Yeung et al., 2004). This ambiguity ultimately reflects the fact that activities from many cortical areas over several cm^2 are irreversibly superimposed at each scalp EEG sensor. The current recordings provide unambiguous localization with spatial accuracy of ~150μ. The observation that the transmembrane currents generating spontaneous and event-related thetas have identical laminar profiles in all five cortical locations is thus very strong evidence that they may indeed be generated by identical synapses. The event-related theta could not be due to superposition of a *de novo* waveform on a constant unrelated background, because in many cases the total theta power decreased after the stimulus, confirming similar observations made previously with intracranial macroelectrodes in humans (Klopp et al., 1999; Rizzuto et al., 2003; Hermes et al., 2013). Furthermore, the post-stimulus theta was strongly phase-locked with the stimulus in inferotemporal and perirhinal areas, and thus would summate across trials to contribute to the ERP. Outside of the ventral temporal neocortex, in entorhinal, prefrontal and cingulate cortices, theta is also modulated by the task, with strong inter-trial coherence mainly in the delta range contributing to the event-related LFP average. This is consistent with suggestions that some midfrontal scalp ERP components arise from phase-locked anterior cingulate theta (Cavanagh et al., 2012). Phase-locking was strong enough to be observed in CSD from individual trials and thus cannot be a statistical artifact. In summary, previous studies have shown that certain ERP components could have resulted from phase-locking of spontaneous activity to stimulus onset, but could not prove it because similar scalp EEG topographies can result from very different brain generator configurations. We show here that indeed, pre-stimulus spontaneous theta and post-stimulus phase-locked theta have identical generators at a very high measurement resolution, and thus most of the ERP is not superimposed *de novo* activity, but identical to spontaneously occurring potentials. Furthermore, the laminar profile of spontaneous theta was also similar to that of the initial feedforward sink, although with a different duration and thus different frequency. Thus, ERP components with frequencies outside the theta range may also be generated by similar neural circuits, implying that theta may reflect the participation of the basic word-understanding circuit in the generation of task-unrelated (i.e., spontaneous) thought, as well as task-provoked sustained processing.

Role of theta in cortical processing

Theta was found to consistently modulate the level of cortical excitability as indexed by population firing and HGP, within the context of a laminar CSD distribution of implying an alternation in the source of predominant cortical input between lower and higher cortical areas (Figure 8). These linked oscillations in excitability and in feedforward/feedback balance may help select a cortical circuit to specifically encode an event.

Anatomical and physiological observations in monkeys suggest that after the first bottom-up sweep of information, local and top-down reactions carry additional inferences and mnestic associations (Lamme and Roelfsema, 2000; Merker, 2004; Burke et al., 2005), as well as predictions for subsequent stimuli (Bastos et al., 2012). Since most cortico-cortical connections are excitatory, inhibition needs to progressively increase to prevent associations from generating runaway excitation (Read et al., 1994), transforming the character of network building from divergent to convergent (Figure 8). Eventually, only the most highly interconnected cortical elements are able to overcome the inhibitory threshold through their mutually-reinforcing interactions.

The feedback connections provide sustained activation that permits converging feedforward excitation to overcome inhibition (Shao and Burkhalter, 1996, 1999), and thus selects the feedforward activity that is consistent with the context (Bastos et al., 2012). Consistent with this view, words may evoke sustained firing in deep layers that persists through the phasic LFPs and firing in middle and upper layers (Halgren et al., 2006). Thus, theta may assist in communication between cortical areas by grouping and synchronizing the processing of inter-related chunks of information, as has been shown to occur in the HC (Jezek et al., 2011; Gupta et al., 2012). Feedback, or especially the interplay of feedforward and feedback, may provide the context to form and recall memories, and the convergence of feedforward and feedback information may play a critical role in plasticity (Larkum, 2013). Therefore, the alternating middle/superficial sink/source dynamics observed here may be a domain general process for the integration of new information into existing context.

The widespread generation of theta is consistent with it representing distributed modulation of cortical network properties. We found, as have others (Canolty et al., 2006), that local theta phase modulates high gamma power. Elegant theories have developed the idea that successive cycles of gamma waves embedded in theta carry different chunks of information during working memory (Jensen and Lisman, 1996; Nyhus and Curran, 2010; Lisman and Jensen, 2013). However, these theories predict gamma oscillations with a consistent frequency, typically ~40Hz, while we observed a broadband increase up to ~200Hz, characteristic of a global increase in synaptic and multiunit activity (Lachaux et al., 2012).

Role of theta in linking hippocampus and AVTL with cortex in declarative memory and word understanding

Hippocampal theta has been intensively studied in rodents to elucidate the neural mechanisms whereby allocentric space and declarative memories are constructed and retrieved (O'Keefe and Nadel, 1978; Burgess and O'Keefe, 2011). Theta modulates hippocampal plasticity (Pavlides et al., 1988), suggesting that it may promote alternating periods of encoding and retrieval (Hasselmo et al., 2002). Theta entrains HC place cell firing with a phase precession that may aid planning and prediction in space (O'Keefe and Nadel, 1978; Burgess and O'Keefe, 2011). Interference between theta waves may help create ER grid cells (Hasselmo and Stern, 2013). Intracranial recordings in humans have found that HC slow theta (~3 Hz) is associated with memory encoding (Fell and Axmacher, 2011; Lega et al., 2011), and a sustained increase in theta lasting seconds occurs in ER during retrieval of recently acquired information (Knake et al., 2007) or remote autobiographical memories

(Steinvorth et al., 2010). Indeed, theta activity has been recorded in many cortical areas during working memory tasks (Halgren et al., 2002a; Raghavachari et al., 2006; Rizzuto et al., 2006).

Neocortical activity is relayed through PR, IT and superficial ER layers to the HC, and deep ER layers receive HC output and relay it back to PR, IT and widespread association cortex (Felleman and VanEssen, 1991; Biella et al., 2002; Insausti and Amaral, 2004). This long feedback loop is crucial to models of memory wherein specific HC connections are formed to encode novel constellations of elements in episodic events, and these connections help guide the retrieval of those constellations at a later time (Halgren, 1984; Alvarez and Squire, 1994; Burke et al., 2005). However, transmission through this multistage path is difficult, low-probability, and requires convergence to be effective (Biella et al., 2002; Pelletier et al., 2004). We observed that the AVTL activity encoding the semantic aspects of words is the first phase of a reset theta. We hypothesize that this theta helps synchronize activity in distant structures to allow distributed networks of mutually excitatory neurons to represent the event with high fidelity (Chrobak and Buzsaki, 1998; von Stein and Sarnthein, 2000; Hasselmo et al., 2002). Consistent with this theory, HC theta in rodents modulates gamma frequency neuronal firing in parietal cortex (Sirota and Buzsaki, 2005)

In the model outlined above, theta orchestrates the alternation of topdown and bottom up processing and thus the cycle of encoding is linked with the cycle of plasticity; specifically theta may function to ensure that memory snapshots are made at the conclusion of encoding during convergent processing when there is both topdown and bottom up activity (Norman et al., 2005; Norman et al., 2007). Sustained firing by event-encoding neurons in the feedforward path will be reinforced (to overcome GABAa inhibition) through feedback during the top-down part of the theta cycle to permit integration with context and formation of memories that unite context with feed-forward input. This is consistent with studies where subsequent memory is not correlated with the N400 but the following component, termed the P600 or Late Positive Component (LPC) (Paller et al., 1988) and the theta (Nyhus and Curran, 2010; Lega et al., 2011). In our recordings, the LPC would correspond to the upper layer sink which follows the middle layer sink associated with the N400, and comprises the feedback phase of the theta rhythm. In language processing, the LPC is elicited when automatic lexico-semantic associations result in erroneous interpretations, such as in puns (Marinkovic et al., 2011)(Kuperberg, 2007; Brouwer et al., 2012).

Role of theta in understanding words in sentences

Outside of the laboratory, words do not usually occur in isolation, but rather in sentences, where they are read or heard at a rate comparable to high delta or low theta. In the model proposed here, each content word would trigger an N400 process that encodes its lexicosemantic content in a first-pass layer IV sink. This sink constitutes the first phase of the reset theta, and at its completion it feeds back to converge in upper layers with other associative input to be integrated into the ongoing cognitive context during the surface negative phase of the theta (Marinkovic et al., 2012). The next word would arrive at the beginning of the next cycle, promoting its integration with the developing sentence context (Giraud and Poeppel, 2012). The network thus created in the first theta cycle would be

highly stable due to recurrent excitation and surround inhibition. The following theta cycle may function to release the network from this local minimum, by redirecting input back toward the periphery, while externally modulating excitability (Figure 8). The successor network would in turn combine its distilled representation with new input to create a new network at each cycle.

These predictions from observations of responses to single words were tested in laminar recordings from PR during the reading of complete sentences. Like the pattern evoked by isolated words, the initial word of sentences evoked a sharp initial middle layer sink, followed by a broader upper layer sink, both accompanied by increased MUA. Furthermore, these patterns were strongly modulated by semantic content, when comparing content versus function words, in a manner similar to that observed for the N400m observed with MEG to function words in sentences {Halgren, 2002 #14057}.

Theta frequency rhythms were entrained by the regular presentation of the words, and continued for a short period after the sentence. A new component of activity was observed to later words in the sentence. This component, an early middle layer sink, arrived about 80-90ms prior to the initial arrival of information from lower cortical areas encoding the current word. Thus, this early peak is organized by the preceding word, but modulates the level of excitability in middle cortical layers just prior to their processing of the current word, as predicted by the model described above.

Conceivably, this modulation could be adjusted to match the word that is expected to follow it. Some function words (such as ‘out’) are usually followed by another function word, whereas other function words (such as ‘the’) are usually followed by a content word. The peak at 40ms was absent to the former, and large to the latter, suggesting that the effect of a word on the neural preparation for the next word following it may be modulated by syntactic probabilities. Although limited to a single subject, these recordings tend to support the prediction that the extended rhythmic responses to a given word sets a neural context for the processing of the next.

Limitations

The certainty and breadth of application of the interpretations offered here are limited by the recordings that were available. Although these laminar recordings of theta activity in humans are unique, only five patients were recorded with single-word tasks, and only one patient with complete sentences. While the main results were qualitatively consistent across subjects (and between single-words vs. complete sentences), the high spatial accuracy of these micro-array recordings means that they are unlikely to be in exactly the corresponding location in different patients, rendering problematic the statistical combining of data across subjects. Thus, we statistically demonstrate effects across repeated measures but within subjects. Access to intracranial recordings are only available in the context of clinical care, in this case the pre-surgical evaluation for epilepsy. While we made every effort to eliminate epochs or electrodes that were overtly contaminated by epileptiform activity, subtle effects of the patients’ pathology or medications cannot be ruled out. We infer the laminar origin and destination of information flow from the known neuroanatomical location of feedforward and other afferents in relationship to the current sinks generating the theta

modulated by word processing. However, tests of information flow between structures that would be enabled by recordings from multiple structures were not possible because only one laminar micro-electrode array was recorded from in each subject. In particular, more distributed micro-array recordings would be needed to establish the precise role of the AVTL in organizing, via the theta rhythm, activity in widespread cortical networks.

Summary

Microelectrode array recordings during word processing demonstrate spontaneous and evoked modulations of the primary source of excitatory inward currents between middle layers receiving feedforward input and upper layers engaging widespread associations. Coordinated with this alternating focus on first-pass template-matching versus internally-generated associations is an alternation of overall excitation driving the network toward divergent versus convergent processing. This oscillation could be used to trigger memory formation when event-encoding is maximally accurate and comprehensive, and then release processing from mutually-reinforcing interactions. In language, theta could optimize the integration of words into the developing sentence context.

Supplementary Material

Refer to Web version on PubMed Central for supplementary material.

Acknowledgements

We thank George Karmos, Howard Blume, Gary Heit, Qianqian Deng, Tristan Davenport, Lucia Melloni, Suresh Narayanan, Julian Wu, and Katherine Reid for their contributions to this research. Supported by ONR MURI N00014-13-1-0672 and NIH NS18741.

References

Alonso, A. Spotlight on neurons (II): electrophysiology of the neurones in the perirhinal and entorhinal cortices and neuromodulatory changes in firing patterns.. In: Witter, MP.; Wouterlood, F., editors. In: The Parahippocampal Region: organization and role in cognitive function. Oxford University Press; Oxford: 2002. p. 89-105.

Alvarez P, Squire L. Memory consolidation and the medial temporal lobe: a simple network model. Proc Natl Acad Sci U S A. 1994; 91:7041–7045. [PubMed: 8041742]

Barbas H, Rempel-Clower N. Cortical structure predicts the pattern of corticocortical connections. Cereb Cortex. 1997; 7:635–646. [PubMed: 9373019]

Bastiaansen M, Hagoort P. Event-induced theta responses as a window on the dynamics of memory. Cortex. 2003; 39:967–992. [PubMed: 14584562]

Bastos AM, Usrey WM, Adams RA, Mangun GR, Fries P, Friston KJ. Canonical microcircuits for predictive coding. Neuron. 2012; 76:695–711. [PubMed: 23177956]

Biella G, Uva L, de Curtis M. Propagation of neuronal activity along the neocortical-perirhinal-entorhinal pathway in the guinea pig. J Neurosci. 2002; 22:9972–9979. [PubMed: 12427854]

Bilkey DK, Heinemann U. Intrinsic theta-frequency membrane potential oscillations in layer III/V perirhinal cortex neurons of the rat. Hippocampus. 1999; 9:510–518. [PubMed: 10560921]

Brouwer H, Fitz H, Hoeks J. Getting real about semantic illusions: rethinking the functional role of the P600 in language comprehension. Brain Res. 2012; 1446:127–143. [PubMed: 22361114]

Brown MW, Aggleton JP. Recognition memory: what are the roles of the perirhinal cortex and hippocampus? Nat Rev Neurosci. 2001; 2:51–61. [PubMed: 11253359]

Burgess N, O'Keefe J. Models of place and grid cell firing and theta rhythmicity. Curr Opin Neurobiol. 2011; 21:734–744. [PubMed: 21820895]

Burke SN, Chawla MK, Penner MR, Corwell BE, Worley PF, Barnes CA, McNaughton BL. Differential encoding of behavior and spatial context in deep and superficial layers of the neocortex. Neuron. 2005; 45:667–674. [PubMed: 15748843]

Buzsaki G. Theta oscillations in the hippocampus. Neuron. 2002; 33:325–340. [PubMed: 11832222]

Canolty RT, Edwards E, Dalal SS, Soltani M, Nagarajan SS, Kirsch HE, Berger MS, Barbaro NM, Knight RT. High gamma power is phase-locked to theta oscillations in human neocortex. Science. 2006; 313:1626–1628. [PubMed: 16973878]

Cavanagh JF, Zambrano-Vazquez L, Allen JJ. Theta lingua franca: a common mid-frontal substrate for action monitoring processes. Psychophysiology. 2012; 49:220–238. [PubMed: 22091878]

Chan AM, Baker JM, Eskandar E, Schomer D, Ulbert I, Marinkovic K, Cash SS, Halgren E. First-pass selectivity for semantic categories in human anteroventral temporal lobe. J Neurosci. 2011; 31:18119–18129. [PubMed: 22159123]

Chan AM, Dykstra AR, Jayaram V, Leonard MK, Travis KE, Gygi B, Baker JM, Eskandar E, Hochberg LR, Halgren E, Cash SS. Speech-Specific Tuning of Neurons in Human Superior Temporal Gyrus. Cereb Cortex. 2013

Chrobak JJ, Buzsaki G. Operational dynamics in the hippocampal-entorhinal axis. Neurosci Biobehav Rev. 1998; 22:303–310. [PubMed: 9579320]

Colgin LL. Mechanisms and functions of theta rhythms. Annu Rev Neurosci. 2013; 36:295–312. [PubMed: 23724998]

Dale AM, Liu AK, Fischl BR, Buckner RL, Belliveau JW, Lewine JD, Halgren E. Dynamic statistical parametric mapping: combining fMRI and MEG for high-resolution imaging of cortical activity. Neuron. 2000; 26:55–67. [PubMed: 10798392]

Delorme A, Makeig S. EEGLAB: an open source toolbox for analysis of single-trial EEG dynamics including independent component analysis. Journal of Neuroscience Methods. 2004; 134:9–21. [PubMed: 15102499]

Dhond RP, Marinkovic K, Dale AM, Witzel T, Halgren E. Spatiotemporal maps of past-tense verb inflection. Neuroimage. 2003; 19:91–100. [PubMed: 12781729]

Fell J, Axmacher N. The role of phase synchronization in memory processes. Nat Rev Neurosci. 2011; 12:105–118. [PubMed: 21248789]

Felleman DJ, VanEssen DC. Distributed hierarchical processing in the primate cerebral cortex. Cerebral Cortex. 1991; 1:1–47. [PubMed: 1822724]

Giraud AL, Poeppel D. Cortical oscillations and speech processing: emerging computational principles and operations. Nature Neuroscience. 2012; 15:511–517. [PubMed: 22426255]

Gupta AS, van der Meer MA, Touretzky DS, Redish AD. Segmentation of spatial experience by hippocampal theta sequences. Nat Neurosci. 2012; 15:1032–1039. [PubMed: 22706269]

Halgren, E. Human hippocampal and amygdala recordings and stimulation: Evidence for a neural model of recent memory.. In: Squire, L.; Butters, N., editors. The Neuropsychology of Memory. Guilford; New York: 1984. p. 165-181.

Halgren, E. Insights from evoked potentials into the neuropsychological mechanisms of reading.. In: Scheibel, A.; Weschsler, A., editors. Neurobiology of Cognition. Guilford; New York: 1990. p. 103-150.

Halgren, E. Considerations in source estimation of the P3.. In: Ikeda, A.; Inoue, Y., editors. Event-related Potentials in Patients with Epilepsy. John Libbey Eurotext; Paris: 2008.

Halgren E, Baudena P, Heit G, Clarke JM, Marinkovic K. Spatio-temporal stages in face and word processing. 1. Depth-recorded potentials in the human occipital, temporal and parietal lobes. Journal of Physiology (Paris). 1994a; 88:1–50.

Halgren E, Boujon C, Clarke J, Wang C, Chauvel P. Rapid distributed fronto-parieto-occipital processing stages during working memory in humans. Cerebral Cortex. 2002a; 12:710–728. [PubMed: 12050083]

Halgren E, Baudena P, Heit G, Clarke JM, Marinkovic K, Chauvel P. Spatio-temporal stages in face and word processing. 2. Depth-recorded potentials in the human frontal and Rolandic cortices. Journal of Physiology (Paris). 1994b; 88:51–80.

Halgren E, Dhond RP, Christensen N, Van Petten C, Marinkovic K, Lewine JD, Dale AM. N400-like magnetoencephalography responses modulated by semantic context, word frequency, and lexical class in sentences. Neuroimage. 2002b; 17:1101–1116. [PubMed: 12414253]

Halgren E, Wang C, Schomer DL, Knake S, Marinkovic K, Wu J, Ulbert I. Processing stages underlying word recognition in the anteroventral temporal lobe. Neuroimage. 2006; 30:1401–1413. [PubMed: 16488158]

Hartwich K, Pollak T, Klausberger T. Distinct firing patterns of identified basket and dendrite-targeting interneurons in the prefrontal cortex during hippocampal theta and local spindle oscillations. J Neurosci. 2009; 29:9563–9574. [PubMed: 19641119]

Harvey CD, Collman F, Dombeck DA, Tank DW. Intracellular dynamics of hippocampal place cells during virtual navigation. Nature. 2009; 461:941–946. [PubMed: 19829374]

Hasselmo ME, Stern CE. Theta rhythm and the encoding and retrieval of space and time. Neuroimage. 2013

Hasselmo ME, Hay J, Ilyn M, Gorchetchnikov A. Neuromodulation, theta rhythm and rat spatial navigation. Neural Netw. 2002; 15:689–707. [PubMed: 12371520]

Heit G, Smith ME, Halgren E. Neural encoding of individual words and faces by the human hippocampus and amygdala. Nature. 1988; 333:773–775. [PubMed: 3386719]

Heit G, Smith ME, Halgren E. Neuronal activity in the human medial temporal lobe during recognition memory. Brain. 1990; 113:1093–1112. [PubMed: 2397384]

Hermes D, Miller KJ, Vansteensel MJ, Edwards E, Ferrier CH, Bleichner MG, van Rijen PC, Aarnoutse EJ, Ramsey NF. Cortical theta wanes for language. Neuroimage. 2013

Hsieh LT, Ranganath C. Frontal midline theta oscillations during working memory maintenance and episodic encoding and retrieval. Neuroimage. 2013

Hunt SMJ. MacProbe: A Macintosh-based experimenter's workstation for the cognitive sciences. Behavioral Research Methods,Instrumentation and Computing. 1994; 26:345–351.

Insausti, AM.; Amaral, DG. Hippocampal Formation.. In: Paxinos, G.; Mai, JK., editors. The Human Nervous System. 2 Edition. Elsevier Academic; San Diego: 2004. p. 871-914.

Jacobs J. Hippocampal theta oscillations are slower in humans than in rodents: implications for models of spatial navigation and memory. Philos Trans R Soc Lond B Biol Sci. 2014; 369:20130304. [PubMed: 24366145]

Jensen O, Lisman JE. Novel lists of 7 +/− 2 known items can be reliably stored in an oscillatory short-term memory network: interaction with long-term memory. Learn Mem. 1996; 3:257–263. [PubMed: 10456095]

Jezek K, Henriksen EJ, Treves A, Moser EI, Moser MB. Theta-paced flickering between place-cell maps in the hippocampus. Nature. 2011; 478:246–249. [PubMed: 21964339]

Jones BE. Activity, modulation and role of basal forebrain cholinergic neurons innervating the cerebral cortex. Prog Brain Res. 2004; 145:157–169. [PubMed: 14650914]

Kamondi A, Acsady L, Wang XJ, Buzsaki G. Theta oscillations in somata and dendrites of hippocampal pyramidal cells in vivo: activity-dependent phase-precession of action potentials. Hippocampus. 1998; 8:244–261. [PubMed: 9662139]

Klimesch W. Memory processes, brain oscillations and EEG synchronization. Int J Psychophysiol. 1996; 24:61–100. [PubMed: 8978436]

Klopp JC, Halgren E, Marinkovic K, Nenov VI. Face-selective event-related spectral changes in the human fusiform gyrus. Clinical Neurophysiology. 1999; 110:677–683.

Knake S, Wang CM, Ulbert I, Schomer DL, Halgren E. Specific increase of human entorhinal population synaptic and neuronal activity during retrieval. Neuroimage. 2007; 37:618–622. [PubMed: 17566769]

Kovacevic S, Azma S, Irimia A, Sherfey J, Halgren E, Marinkovic K. Theta oscillations are sensitive to both early and late conflict processing stages: effects of alcohol intoxication. PLoS ONE. 2012; 7:e43957. [PubMed: 22952823]

Kuperberg GR. Neural mechanisms of language comprehension: challenges to syntax. Brain Res. 2007; 1146:23–49. [PubMed: 17400197]

Kutas M, Federmeier KD. Thirty years and counting: finding meaning in the N400 component of the event-related brain potential (ERP). Annu Rev Psychol. 2011; 62:621–647. [PubMed: 20809790]

Lachaux JP, Rodriguez E, Martinerie J, Varela FJ. Measuring phase synchrony in brain signals. Hum Brain Mapp. 1999; 8:194–208. [PubMed: 10619414]

Lachaux JP, Axmacher N, Mormann F, Halgren E, Crone NE. High-frequency neural activity and human cognition: Past, present and possible future of intracranial EEG research. Prog Neurobiol. 2012; 98:279–301. [PubMed: 22750156]

Lamme VA, Roelfsema PR. The distinct modes of vision offered by feedforward and recurrent processing. Trends Neurosci. 2000; 23:571–579. [PubMed: 11074267]

Larkum M. A cellular mechanism for cortical associations: an organizing principle for the cerebral cortex. Trends in Neurosciences. 2013; 36:141–151. [PubMed: 23273272]

Lega BC, Jacobs J, Kahana M. Human hippocampal theta oscillations and the formation of episodic memories. Hippocampus. 2011

Leonard MK, Ferjan Ramirez N, Torres C, Travis KE, Hatrak M, Mayberry RI, Halgren E. Signed words in the congenitally deaf evoke typical late lexicosemantic responses with no early visual responses in left superior temporal cortex. J Neurosci. 2012; 32:9700–9705. [PubMed: 22787055]

Link A, Elster C, Sander T, Lueschow A, Curio G, Trahms L. MEG-analysis using the Hilbert transform. Biomed Tech (Berl). 2002; 47(Suppl 1)(Pt 2):577–580. [PubMed: 12465242]

Lisman JE, Jensen O. The theta-gamma neural code. Neuron. 2013; 77:1002–1016. [PubMed: 23522038]

Makeig S, Westerfield M, Jung TP, Enghoff S, Townsend J, Courchesne E, Sejnowski TJ. Dynamic brain sources of visual evoked responses. Science. 2002; 295:690–694. [PubMed: 11809976]

Marinkovic K, Rosen BQ, Cox B, Kovacevic S. Event-Related Theta Power during Lexical-Semantic Retrieval and Decision Conflict is Modulated by Alcohol Intoxication: Anatomically Constrained MEG. Frontiers in psychology. 2012; 3:121. [PubMed: 22536192]

Marinkovic K, Dhond RP, Dale AM, Glessner M, Carr V, Halgren E. Spatiotemporal dynamics of modality-specific and supramodal word processing. Neuron. 2003; 38:487–497. [PubMed: 12741994]

Marinkovic K, Baldwin S, Courtney MG, Witzel T, Dale AM, Halgren E. Right hemisphere has the last laugh: neural dynamics of joke appreciation. Cogn Affect Behav Neurosci. 2011; 11:113–130. [PubMed: 21264646]

Merker B. Cortex, countercurrent context, and dimensional integration of lifetime memory. Cortex. 2004; 40:559–576. [PubMed: 15259333]

Mitzdorf U. Current source-density method and application in cat cerebral cortex: investigation of evoked potentials and EEG phenomena. Physiol Rev. 1985; 65:37–100. [PubMed: 3880898]

Nicholson C, Freeman JA. Theory of current source density analysis and determination of the conductivity tensor for anuran cerebellum. Journal of Neurophysiology. 1975; 38:356–368. [PubMed: 805215]

Nobre AC, McCarthy G. Language-related field potentials in the anterior-medial temporal lobe: II. Effects of word type and semantic priming. J Neurosci. 1995; 15:1090–1098. [PubMed: 7869085]

Norman KA, Newman EL, Perotte AJ. Methods for reducing interference in the Complementary Learning Systems model: oscillating inhibition and autonomous memory rehearsal. Neural Netw. 2005; 18:1212–1228. [PubMed: 16260116]

Norman KA, Newman EL, Detre G. A neural network model of retrieval-induced forgetting. Psychol Rev. 2007; 114:887–953. [PubMed: 17907868]

Nyhus E, Curran T. Functional role of gamma and theta oscillations in episodic memory. Neurosci Biobehav Rev. 2010; 34:1023–1035. [PubMed: 20060015]

O'Keefe, J.; Nadel, L. The Hippocampus as a Cognitive Map. Oxford; Clarendon: 1978.

Paller KA, McCarthy G, Wood CC. ERPs predictive of subsequent recall and recognition performance. Biol Psychol. 1988; 26:269–276. [PubMed: 3207786]

Patterson K, Nestor PJ, Rogers TT. Where do you know what you know? The representation of semantic knowledge in the human brain. Nat Rev Neurosci. 2007; 8:976–987. [PubMed: 18026167]

Pavlides C, Greenstein YJ, Grudman M, Winson J. Long-term potentiation in the dentate gyrus is induced preferentially on the positive phase of theta-rhythm. Brain Research. 1988; 439:383–387. [PubMed: 3359196]

Pelletier JG, Apergis J, Pare D. Low-probability transmission of neocortical and entorhinal impulses through the perirhinal cortex. J Neurophysiol. 2004; 91:2079–2089. [PubMed: 15069098]

Pignatelli M, Beyeler A, Leinekugel X. Neural circuits underlying the generation of theta oscillations. Journal of physiology, Paris. 2012; 106:81–92.

Raghavachari S, Lisman JE, Tully M, Madsen JR, Bromfield EB, Kahana MJ. Theta oscillations in human cortex during a working-memory task: evidence for local generators. J Neurophysiol. 2006; 95:1630–1638. [PubMed: 16207788]

Read W, Nenov V, Halgren E. Role of inhibition in memory retrieval by hippocampal area CA3. Neurosci Biobehav. 1994; 18:55–68.

Rizzuto DS, Madsen JR, Bromfield EB, Schulze-Bonhage A, Kahana MJ. Human neocortical oscillations exhibit theta phase differences between encoding and retrieval. Neuroimage. 2006; 31:1352–1358. [PubMed: 16542856]

Rizzuto DS, Madsen JR, Bromfield EB, Schulze-Bonhage A, Seelig D, Aschenbrenner-Scheibe R, Kahana MJ. Reset of human neocortical oscillations during a working memory task. Proc Natl Acad Sci U S A. 2003; 100:7931–7936. [PubMed: 12792019]

Salin PA, Bullier J. Corticocortical connections in the visual system: structure and function. Physiol Rev. 1995; 75:107–154. [PubMed: 7831395]

Shao Z, Burkhalter A. Different balance of excitation and inhibition in forward and feedback circuits of rat visual cortex. J Neurosci. 1996; 16:7353–7365. [PubMed: 8929442]

Shao Z, Burkhalter A. Role of GABAB receptor-mediated inhibition in reciprocal interareal pathways of rat visual cortex. J Neurophysiol. 1999; 81:1014–1024. [PubMed: 10085329]

Sirota A, Buzsaki G. Interaction between neocortical and hippocampal networks via slow oscillations. Thalamus Relat Syst. 2005; 3:245–259. [PubMed: 18185848]

Sirota A, Montgomery S, Fujisawa S, Isomura Y, Zugaro M, Buzsaki G. Entrainment of neocortical neurons and gamma oscillations by the hippocampal theta rhythm. Neuron. 2008; 60:683–697. [PubMed: 19038224]

Smith ME, Stapleton JM, Halgren E. Human medial temporal lobe potentials evoked in memory and language tasks. Electroenceph Clin Neurophysiol. 1986; 63:145–159. [PubMed: 2417815]

Snider J, Plank M, Lynch G, Halgren E, Poizner H. Human cortical theta during free exploration encodes space and predicts subsequent memory. J Neurosci. 2013; 33:15056–15068. [PubMed: 24048836]

Steinvorth S, Wang C, Ulbert I, Schomer D, Halgren E. Human entorhinal gamma and theta oscillations selective for remote autobiographical memory. Hippocampus. 2010; 20:166–173. [PubMed: 19338019]

Talairach, J.; Tournoux, P. Co-Planar Stereotaxic Atlas Of The Human Brain. Thieme Medical Publishers; New York: 1988.

Thesen T, McDonald CR, Carlson C, Doyle W, Cash S, Sherfey J, Felsovalyi O, Girard H, Barr W, Devinsky O, Kuzniecky R, Halgren E. Sequential then interactive processing of letters and words in the left fusiform gyrus. Nat Commun. 2012; 3:1284. [PubMed: 23250414]

Thomson AM, Bannister AP. Interlaminar connections in the neocortex. Cereb Cortex. 2003; 13:5–14. [PubMed: 12466210]

Travis KE, Leonard MK, Brown TT, Hagler DJ Jr. Curran M, Dale AM, Elman JL, Halgren E. Spatiotemporal neural dynamics of word understanding in 12- to 18-month-old-infants. Cereb Cortex. 2011; 21:1832–1839. [PubMed: 21209121]

Travis KE, Leonard MK, Chan AM, Torres C, Sizemore ML, Qu Z, Eskandar E, Dale AM, Elman JL, Cash SS, Halgren E. Independence of early speech processing from word meaning. Cereb Cortex. 2013; 23:2370–2379. [PubMed: 22875868]

Ulbert I, Halgren E, Heit G, Karmos G. Multiple microelectrode - recording system for human intracortical applications. Journal of Neuroscience Methods. 2001; 106:69–79. [PubMed: 11248342]

von Stein A, Sarnthein J. Different frequencies for different scales of cortical integration: from local gamma to long range alpha/theta synchronization. Int J Psychophysiol. 2000; 38:301–313. [PubMed: 11102669]

Wang C, Ulbert I, Schomer DL, Marinkovic K, Halgren E. Responses of human anterior cingulate cortex microdomains to error detection, conflict monitoring, stimulus-response mapping, familiarity, and orienting. J Neurosci. 2005; 25:604–613. [PubMed: 15659596]

Watrous AJ, Lee DJ, Izadi A, Gurkoff GG, Shahlaie K, Ekstrom AD. A comparative study of human and rat hippocampal low-frequency oscillations during spatial navigation. Hippocampus. 2013; 23:656–661. [PubMed: 23520039]

Yeung N, Bogacz R, Holroyd CB, Cohen JD. Detection of synchronized oscillations in the electroencephalogram: An evaluation of methods. Psychophysiology. 2004; 41:822–832. [PubMed: 15563335]

Yoshimura Y, Dantzker JL, Callaway EM. Excitatory cortical neurons form fine-scale functional networks. Nature. 2005; 433:868–873. [PubMed: 15729343]

Highlights

We used microelectrode arrays to define the circuits generating theta in humans.

Theta was generated by excitation alternating between input and association layers.

Baseline and word-evoked theta have the same generators.

Cognitive event-related potentials may represent reset theta.

Theta may help support extended and widespread cognitive processing.

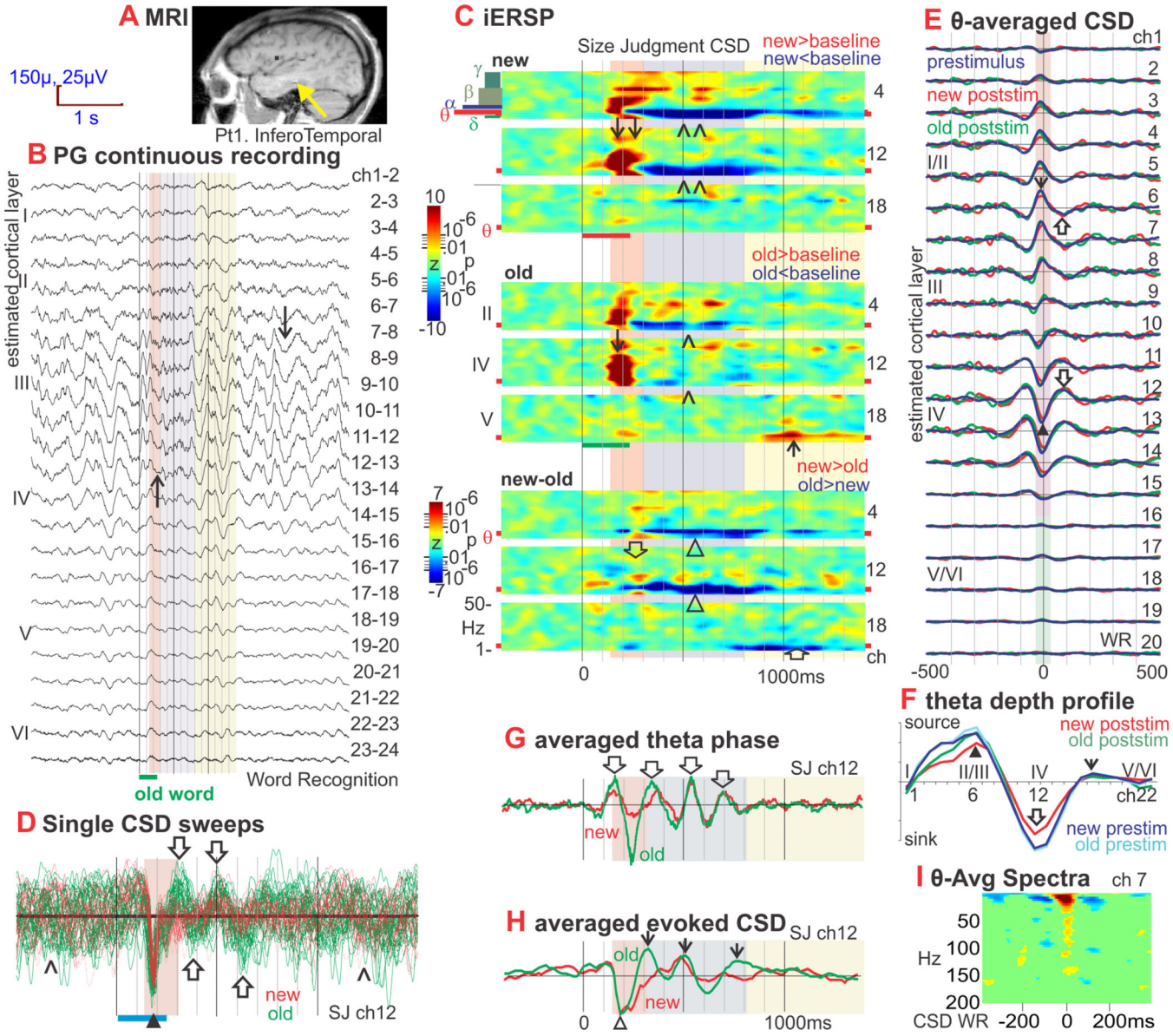

Figure 1. Inferotemporal (IT) theta: generation, task-modulation, phase-resetting, and comparison of spontaneous and event-related. Add average CSD map to show that initial sink is same as theta but different frequency. Move modulation of information specificity to show that maximum encoding happens during upper level sink

A. Location of the linear microelectrode array in anteroventral IT is indicated with a yellow arrowhead on a sagittal MRI taken with the electrodes *in situ*. The probe is in the lateral aspect of the fusiform g., medial bank of lateral occipito-temporal s. (coordinates 38 lateral, 22 posterior, 11 down) (Talairach and Tournoux, 1988). Patient 1.

B. Potential gradient (PG) recorded between contacts at 150µ centers, during 2 Word Recognition trials (WR). Spontaneous background activity between trials is dominated by 4-5 Hz oscillations (↓) in middle to upper cortical layers (channels 6 to 14, periods with white background). Presentation of new or old words (red and green bars at bottom)

suppresses the theta activity (↑), especially from ~300-800ms after word onset (periods with violet background).

C. iERSP plotted as a z-score relative to the pre-stimulus baseline for each frequency and channel, allowing the task-related modulation of theta to be examined and compared to other frequencies. In the **new** and **old** plots, the values are averaged across trials and Red indicates increases in CSD power in that frequency, latency and channel from baseline; blue indicates a decrease. In the **new-old** plots, iERSP is expressed as a t-test between trials with new versus old words. Red indicates more power to new than old words in that frequency, latency and channel; blue indicates less. Data is presented from a Size Judgment (SJ) task to words referring to objects or animals. Similar results were obtained in WR (see Figure S1e), and a Verb Conjugation task where the subject detects regular past tense morphology (not shown). The initial response is a strong wideband increase in spectral power at ~130-300ms (pink background) in upper and especially middle layers (↓). New and Old are initially similar, but significantly diverge starting ~230ms, when the spectral power increase to the Olds abruptly ends, whereas that to the News continues until ~300ms (↓↓) resulting in significant new/old differences (⇓). During the next phase, lasting until ~800ms post-stimulus onset (violet background), theta activity profoundly decreases compared to baseline (^). The decrease is deeper to new words (^^) resulting in significant new/old differences (Δ). In the third phase, until ~1400ms (yellow background), theta increases in deep layers to old words (↑), resulting in significant old>new differences (⇑). The overall pattern of response as well as the effects of word repetition were similar in all tasks, regardless of whether repetition defined explicit recognition targets, or was incidental to task requirements.

D. Middle layer CSD waveforms from individual trials aligned on stimulus onset and superimposed. In the pre-stimulus period, the CSD is large, and dominated by low frequencies with no discernable phase-relationship (^). This activity is abruptly terminated by a sharp current sink (downward deflections) peaking at ~180ms (▲), evolving into synchronous theta oscillations (⇑⇓) that are more prominent for old (green, 31 trials) than new words (red, 23 trials). The sharp peak is ~65ms duration, corresponding to ~16 Hz. Theta source peaks are visible at ~300, ~500 and ~700ms, after which the theta rapidly loses its phase-locking with the stimulus. Raw waveforms were high pass filtered at 1 Hz. Trials were selected for display that evoked a large amplitude initial sink from 170 to 200ms on ch 12.

E. Laminar profile of theta-generating transmembrane current flows. CSD amplitude is plotted against time to show average waveforms of theta cycles in different cortical layers. These demonstrate that theta is generated by sinks in middle cortical layers, (▲; purple box) accompanied by sources in more superficial (↓; orange box) and (weakly) in deep layers (green box). Over time, these alternate with sources in middle layers (⇓) and sinks (⇑) in superficial and (weakly) deep layers. Separate waveforms are shown for the second through fourth theta cycles after old (green) or new (red) word presentation (these occurred approximately in the range of 300-800ms after word onset), and for the second through fourth theta cycles prior to the stimulus (blue). Amplitude profiles of the three waveforms across cortical layers are indistinguishable, implying that event-related and spontaneous thetas are generated by similar or identical intracolumnar synaptic circuitry. Theta is

generated through alternating sources and sinks in middle and superficial cortical layers with accompanying sources in superficial and deep layers.

F. CSD amplitude plotted against cortical depth at the trigger time in Figure 1E. The most prominent features of theta generation are a middle layer sink (▲) with superficial (⇓) and deep sources (↓). No difference can be observed between the amplitude profiles of theta generated after the stimulus to new (red) or old (green) words, versus spontaneous theta in the prestimulus period (blue).

G. Theta phase (from the Hilbert transform) averaged with respect to stimulus onset, demonstrating phase-locking with trial onset. Middle-layer phase shows positive peaks at ~140, 340 and 540ms (⇓) after stimulus onset, i.e., at 5Hz. Phase becomes random after ~800ms. Prestimulus phase is also random and thus averages to zero. Note that the Hilbert phase is a nonlinear measure because it abruptly transitions from $-\pi$ to $+\pi$, and thus may appear slightly different from the ITC measure.

H. Event-related averaged CSD. As reported elsewhere (Halgren et al., 2006), the initial response is a sink in layer IV at ~180ms (△). Phase-resetting aligns the CSD waves so that traditional averaging methods reveal an evoked response that includes strong theta frequency oscillations (↓) even though theta power has decreased from the pre-stimulus period.

I. Spectral power, averaged on the peak of the sink in Layer III, increases in a wide band up to ~150Hz. Scale same as C except pixels with zscore less than 3 have been masked as green.

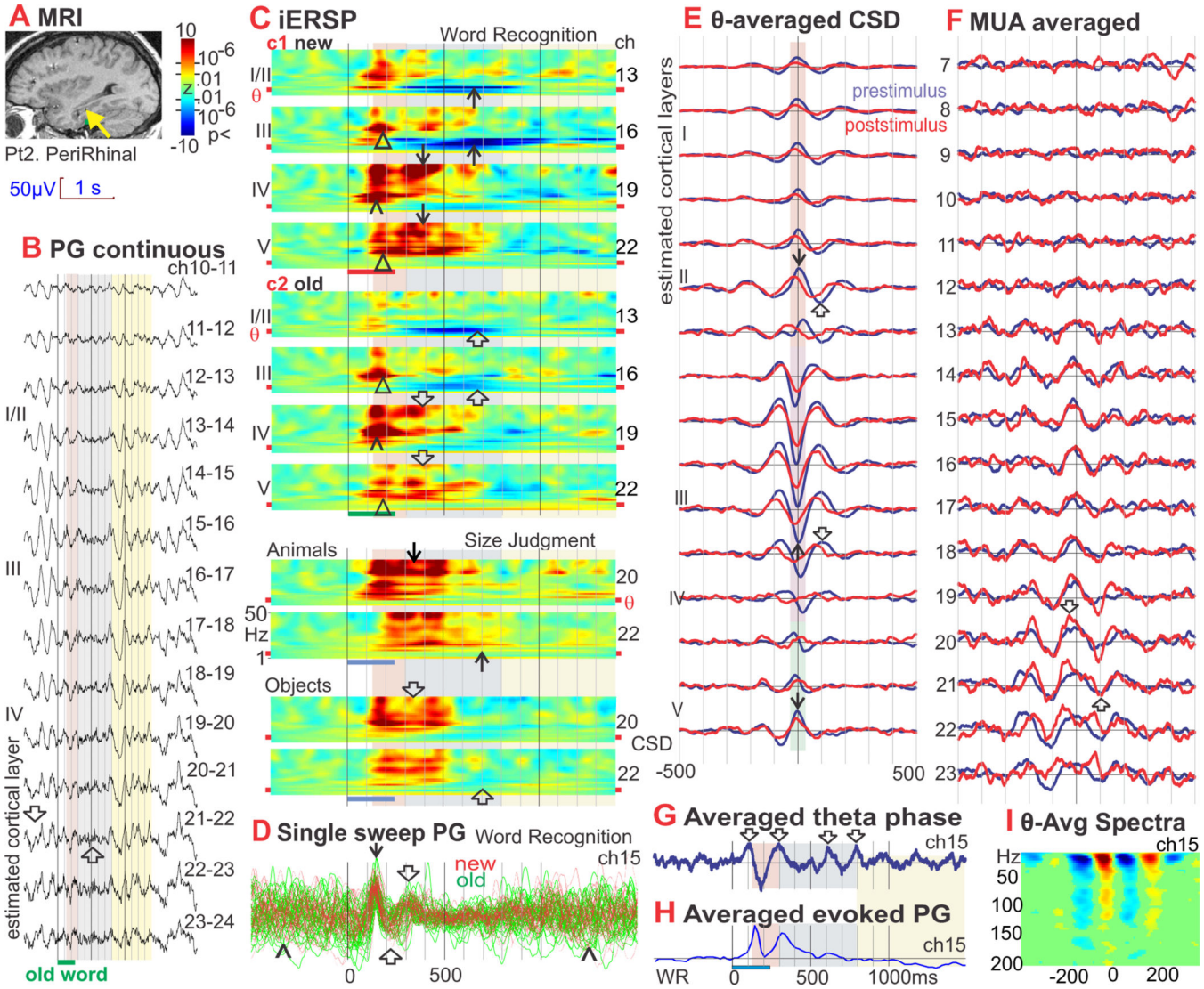

Figure 2. Perirhinal (PR) theta: generation, task-modulation, phase-resetting, and comparison of spontaneous and event-related

A. Yellow arrow indicates the laminar probe location in a sagittal MRI taken with the probes *in situ*. Patient 2, perirhinal cortex (PR): laminar tip in the lateral aspect of the parahippocampal g., medial bank of collateral s. (Talairach coordinates 31, −22, −16).

B. Continuous PG recording during explicit memory (WR). Spontaneous background activity between trials (white background) shows large 4-6 Hz oscillations (↓). Presentation of words suppresses theta (↑), especially from ~300-800ms (periods marked with violet backgrounds).

C. iERSP evoked by words in the WR (above) and SJ (below) tasks. The initial response is a strong broadband increase from ~130-300ms (pink background), that is earliest and strongest in putative layer IV (^), but rapidly spreads to superficial and deep layers (Δ). This initial burst is followed by sustained broadband activity until ~700-800ms, especially in middle and deep layers (↓⇓), and theta in upper layers decreases compared to baseline (↑⇑). The later part of the broadband increase is larger to new words, as is the theta decrease (↓↑).

Similar iERSP patterns are evoked by words referring to animals versus objects in the SJ task. The initial broadband increase in PR spectral power is stronger to animals (↓) than to objects (⇓), as is the subsequent increase in theta (↑⇑).

D. Recordings from single trials, aligned on stimulus onsets and superimposed. Large theta activity with random phase is visible as the thick cloud of traces in the pre-stimulus period and again more than 1200ms after the stimulus (^). Stimulus onset evokes a sharp deflection peaking at ~140ms in the middle cortical layers (↓). The sharp peak is ~80ms duration, corresponding to ~13 Hz. This is followed by a slower oscillation (⇑⇓) from ~200-400ms (~200ms duration, corresponding to ~5Hz, i.e., theta). Overall activity remains suppressed until ~700ms, then gradually recovers by ~1200ms. During this recovery, theta, although small, appears to be synchronized in the superimposed single sweeps. Data is highpass filtered at 1 Hz, and includes 36 trials of old words (green) and 36 of new (red).

E. CSD averaged with respect to theta phase peaks identified using the Hilbert transform. The dominant CSD during theta in PR is a sink (↑) in middle cortical layers III/IV (purple box), with an accompanying source (↓) in layers I/II (orange box) and V (green box). These alternate at theta frequency with sources (⇓) and sinks (⇑) in the corresponding layers. CSD laminar profiles were compared between theta cycles prior (blue traces) versus after the stimulus (red traces). No significant difference was detected between the generating profiles of spontaneous prestimulus and event-related poststimulus theta rhythms.

F. MUA recorded simultaneously and with the same contacts as the CSD in panel **a**. Firing in supragranular, granular and infragranular layers increases during the middle layer sink (⇓), and decreases during the middle layer source (⇑). Thus, the middle layer sink in panel **a** probably represents an EPSC rather than a passive current return.

G. Averaged theta phase. Phase in the theta range from the Hilbert transform is averaged with respect to stimulus onset. Peaks at ~100, 300, 600 and 800ms (⇓) indicate phase-resetting of theta activity by word onset.

H. Average evoked PG response. Phase-resetting results in averaging being able to reveal an evoked response, despite the strong decrease in overall LFP amplitude.

I. Spectral power, averaged on the peak of the sink in Layer III, increases in a wide band up to ~150Hz. Scale same as C except pixels with zscore less than 3 have been masked as green.

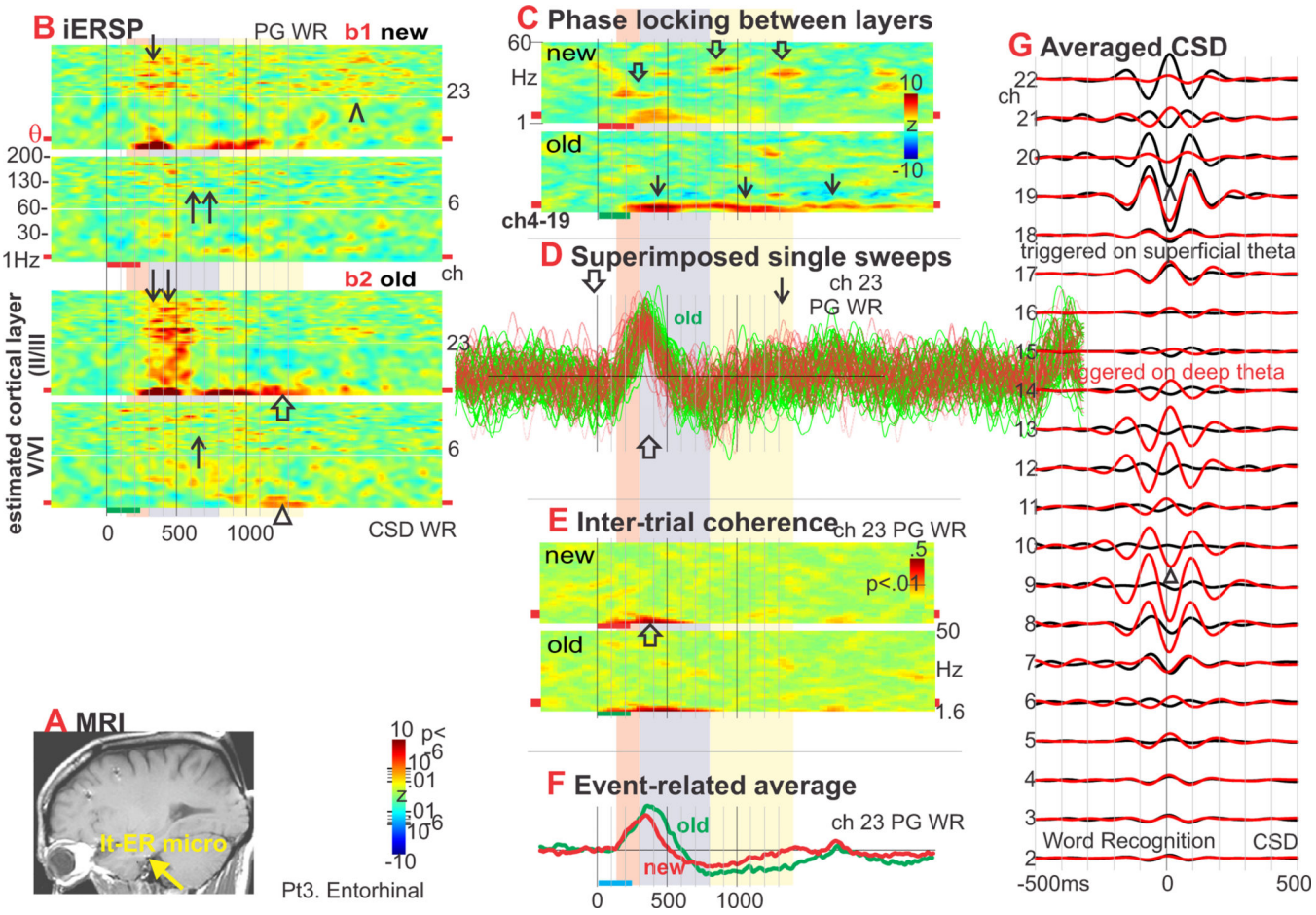

Figure 3. Entorhinal (ER) theta generation and modulation

A. Yellow arrow indicates the entorhinal cortex (ER) laminar probe location on a sagittal MRI taken with the probes *in situ* (Patient 3). Laminar tip is in the medial aspect of the left parahippocampal g., adjacent to the cisterna ambiens (Insausti and Amaral, 2004) (coordinates −23, −17, −25).

B. iERSP evoked in the WR task. Initially, words evoke strong wideband (~2-200Hz) increases in spectral power (↓). The increase is present in both superficial and deep layers, to both new and old stimuli, but is strongest in superficial layers to old words (↓↓). In most frequencies, the broadband increase appears to begin at ~300ms after word onset. Significant old> new differences are present in all frequency bands from ~400-600ms after word onset, mainly in superficial layers. This broadband increase is followed by a theta band increase, from ~500-1100ms in upper layers, new (↑) greater than old (↑↑). At still longer latencies, after 1100ms, theta is larger to old stimuli in both superficial (⇑) and deep layers (Δ). Although the first burst of high frequency activity is mainly to old words and over by ~600ms, high frequency activity continues, especially to new words, until ~2000ms (^).

C. Phase-locking between superficial and deep CSD. Phase locking increases mainly in gamma frequencies to new words (⇓), and mainly in theta and delta bands to old words (↓).

D. PG waveforms from individual trials of WR, aligned on stimulus onset and superimposed. Single trials show an initial component with duration of ~400ms peaking at ~300ms (⇓), followed by a slower components with peaks at ~750ms (⇑) and 1700ms (↓).
E. Inter-Trial Coherence of PG in putative deep ER layer. ITC in low theta and delta frequencies increases relative to baseline until ~900ms after stimulus onset (⇑).
F. Event-related averaged PG during WR. Phase-synchronization of low frequency PG waveforms allows them to contribute to the cross-trial average.
G. Depth profile of the theta CSD. Broadband CSD was averaged to theta peaks found in the band-passed data. Distinct profiles are observed for theta triggered to peaks in the superficial (red traces) versus deep (black traces) layers. In both cases, there are two spatially separated sinks, one deep (Δ) and one superficial (^), with each sink surrounded by its own current sources.

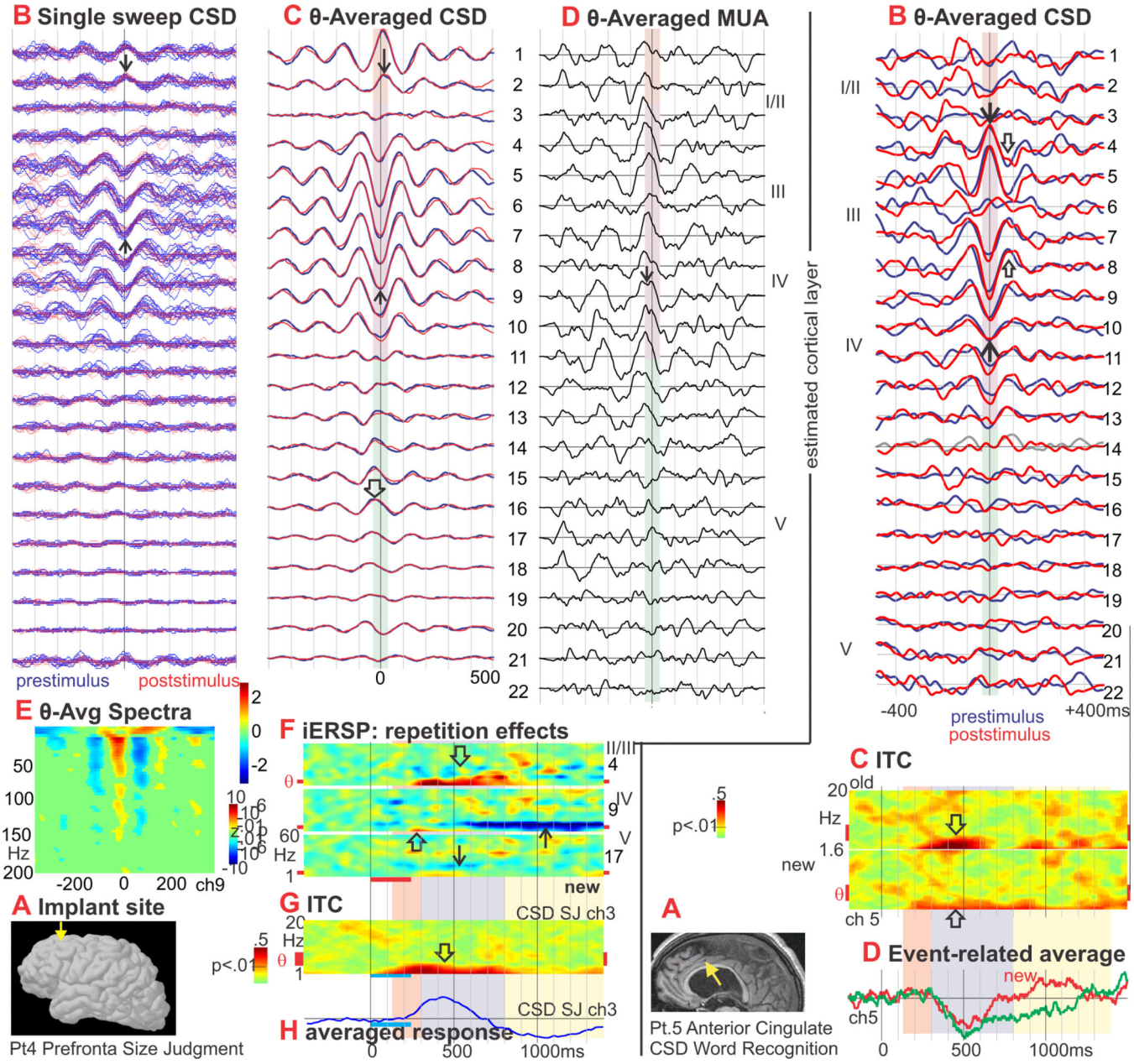

Figure 4. Prefrontal (PF) theta generation and modulation

A. Approximate location of the laminar probe in the left superior prefrontal cortex (↓). Pt. 4.

B. Single sweeps of CSD from all channels, aligned on theta peaks. No differences are visible in the theta bursts from prestimulus (blue traces) versus poststimulus (red traces). Middle layer sinks (↑) and superficial sources (↓) are clearly visible in single sweeps.

C. CSD averaged with respect to theta peaks. The dominant CSD during theta is a middle layer sink (↑) paired with more superficial (↓) and deep (⇓) sources. These alternate with a middle layer source and superficial/deep sinks. No significant difference was detected between the generating profiles of spontaneous prestimulus (blue traces) and event-related poststimulus (red traces) theta rhythms.

D. MUA triggered simultaneously with the CSD in C shows increased neuronal firing across multiple cortical layers during the middle layer sink (↓).

E. Spectral power, averaged on the peak of the sink in Layer III, increases in a wide band up to ~150Hz.

F. iERSP evoked by new words in SJ. A delta-theta range increase begins at ~250ms and is most prominent in upper layers (⇓), but also occurs in middle (⇑) and deep layers (↓). In upper layers the theta continues to more than 900ms, and grows in the alpha range (⇓). In middle layers, the theta increase is followed by a decrease from ~600ms (↑). Unlike temporal lobe sites, no early broadband activation was evoked by words.

G. ITC shows increases in the low theta and delta frequencies relative to baseline from ~100-800ms after stimulus onset (⇑).

H. Event-related CSD average shows mainly delta frequencies.

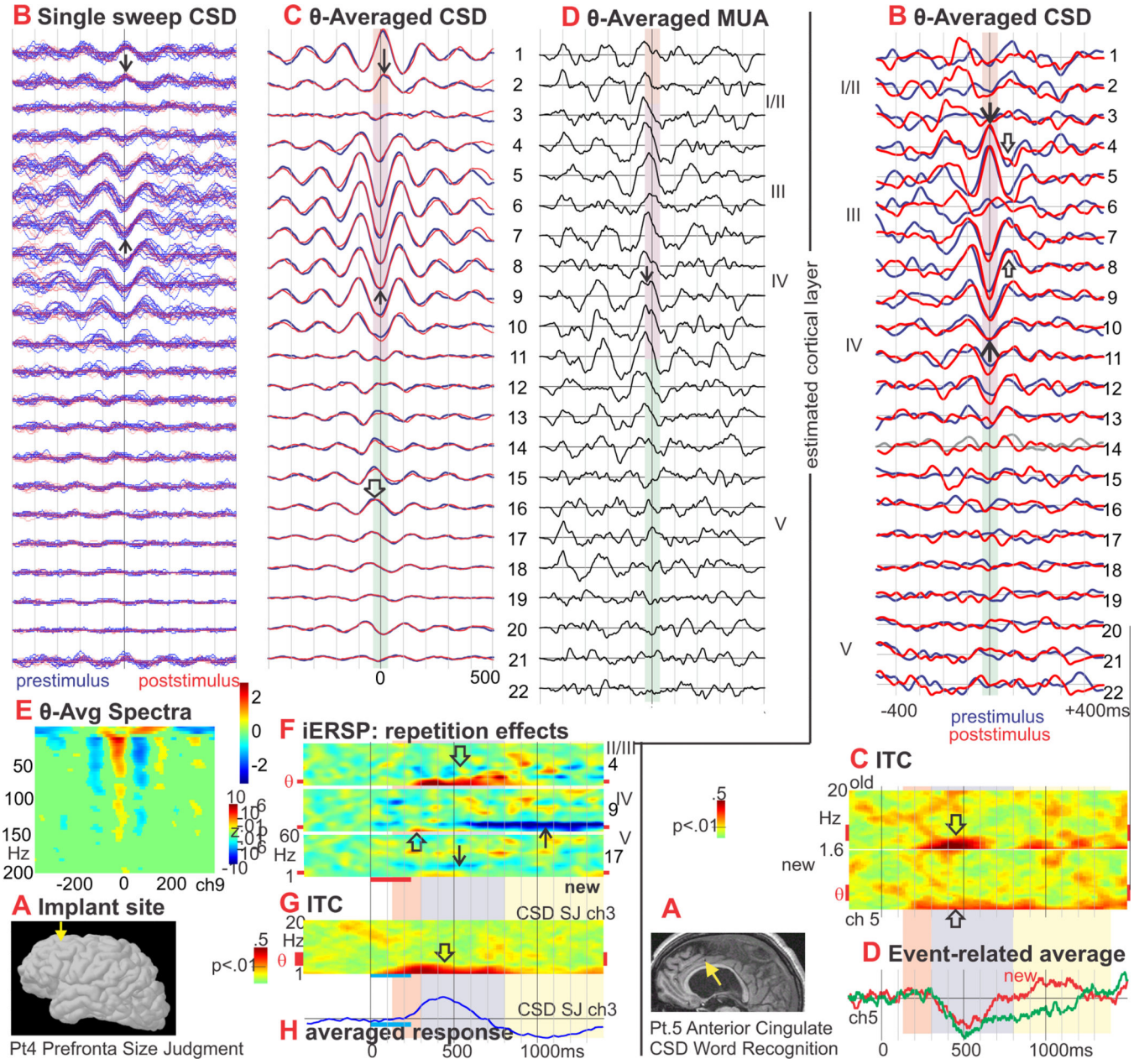

Figure 5. Anterior Cingulate (AC) theta activity

A. Yellow indicates the tip of the right AC laminar probe in approximately Brodmann area 24b' on a mid-sagittal MRI taken with the probes *in situ* (Pt 5). The third ventricle is dilated due to compensated aqueductal stenosis.

B. Laminar distribution of Theta. Broadband CSD averaged with respect to theta peaks. The dominant CSD during theta is a middle layer sink (↑) paired with more superficial source (↓). These alternate with a middle layer source (⇑) and superficial sinks (⇓). No significant difference was detected between the generating profiles of spontaneous prestimulus (blue traces) and event-related poststimulus (red traces) theta rhythms.

C. Inter-Trial Coherence shows increases in the delta frequencies relative to baseline from ~200-900ms after stimulus onset to old (⇓) and new words (⇑).

D. Event-related average shows mainly a delta frequency response.

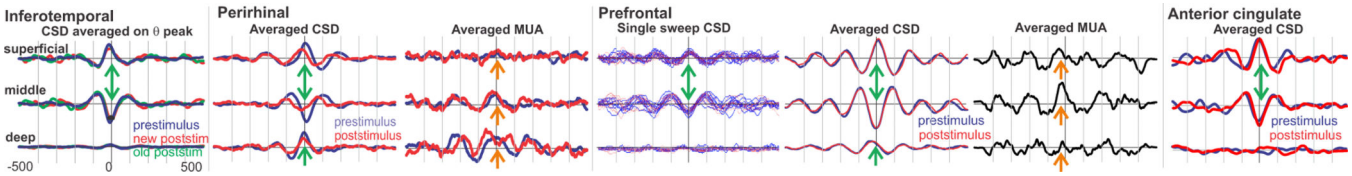

Figure 6. Consistency of theta generation across cortical locations

CSD, averaged on the peak of the theta rhythm, shows that in all 4 cortical areas, the main currents generating the theta are a middle layer sink paired with a superficial source and a weaker deep source. Correlated increases in MUA (in two areas) imply that the sink is active excitation. Spontaneous (prestimulus) and evoked (poststimulus) theta distributions are identical, demonstrating that their neural generators are the same at a microphysiological level. Recordings from each cortical area was obtained in a different 4 subject.

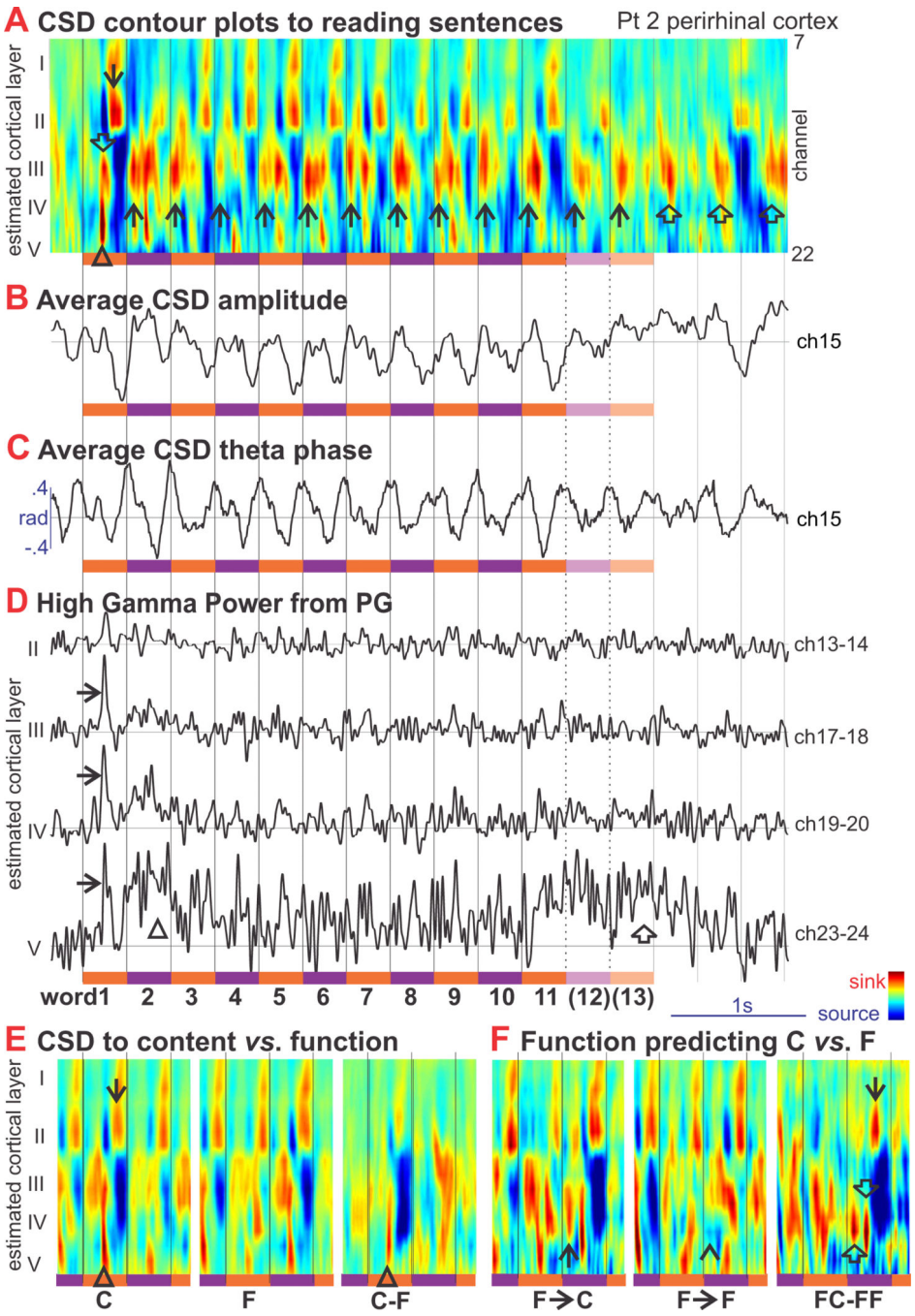

Figure 7. Sentence Reading

A. Average sinks (red) and sources (blue) in different cortical layers are plotted against time during sentence reading. Orange and violet bars indicate the times of the individual words; Black vertical lines indicate word onsets. The initial word evokes a prominent layer IV sink (Δ, onset ~130ms, peak ~150ms) which overlaps with a slightly later layer III sink (⇓, peak ~160ms), followed by sinks in layers I and II (↓) from ~200-290ms. Responses to later words are similar except for a much attenuated initial layer IV sink. Sentences contained either 11 or 13 words. Rhythmic transmembrane currents continue after the sentence (⇑).

Note that there is a consistent layer III/IV sink (↑) occurring to all words except the initial, at ~40ms, *prior* to the arrival of information from the current word.

B. Average CSD amplitude from one channel of the recording in panel A.

C. Average phase from 3 to 7 Hz of the CSD, showing phase-locking of theta to the word-presentation frequency.

D. High gamma power (HGP) in different cortical layers during sentence reading. The initial word evokes a sharp peak ([g314]) indicating increased firing at the same time as the layer IV sink (onset ~130ms, peak ~150ms). This sharp initial peak is also present in other layers, at slightly longer latencies, and is followed by a broad increase in firing from ~300-700ms (△). Sustained firing is also seen at the end of the sentence (⇑), confined to layer V.

E. Average CSD in different cortical layers evoked by Content versus Function words in sentences are compared. The initial layer II/IV sink (Δ) as well as the following I/II sink (↓) are larger to Content words.

F. Average CSD evoked by Function words that are commonly followed by Content versus Function words. Following the function words that predict content words, but prior to the arrival of neural information from the content word, there is a layer III/IV sink (↑) that is absent to words that follow function words which predict other functions words (^). This 'predictive sink' is visible (⇑, peak ~50ms) in the subtraction of the CSD evoked by the two conditions (FC-FF), as are the later evoked sinks in layers IV (⇓, peak ~150ms), and II (↓, peak ~220ms).

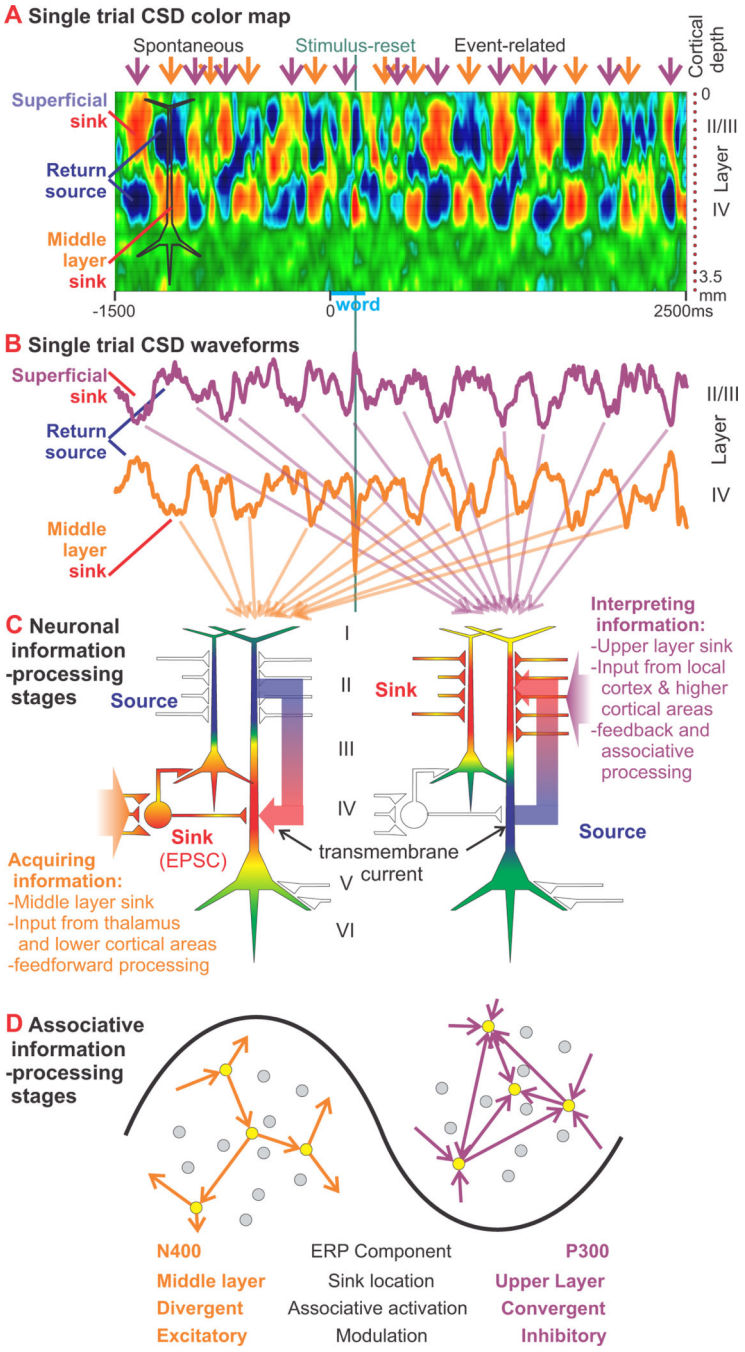

Figure 8. Interpretation of CSD theta oscillations as information-processing stages

A. Sinks (red) and sources (blue) in different cortical layers are plotted against time for a single trial of the SJ task in Pt 1. Periods with superficial sinks and middle layer return sources (purple arrows) alternate with periods of superficial sources and middle layer sinks (orange arrows). Spontaneous oscillations preceding the stimulus are interrupted and reset by a sharp middle layer sink peaking ~200ms after word onset. After the stimulus, the laminar distribution of event-related sinks and sources resembles that of the spontaneous activity.

B. Waveforms from two of the channels (4 and 13) that were used to create the CSD color map in **A** illustrate the alternating sinks and sources in middle and superficial layers.
C. Schematic neurons showing the relationship hypothesized between CSD sinks and synaptic activity. The middle layer sink (left) is interpreted as excitatory feedforward synapses (EPSCs) from lower cortical areas, whereas the superficial sink (right) is interpreted as feedback synaptic activity from higher cortical areas as well as local associative input. CSD estimates transmembrane current, shown entering the cell at the sites of the EPSCs (white plus signs).
D. Consistent with the location of the EPSCs closer to the soma, the middle layer sink is associated with increased population neuronal firing. The spread of new information from lower cortical areas may be facilitated by relative excitatory modulation (left). Over time, as the network becomes increasingly dominated by local and distant feedback associations (right), relative inhibitory modulation requiring convergent activation would prevent run-away excitation.